1982

Lifetime measurements of some S and D states of Cs I.

William S. Neil
University of Windsor

CANADIAN THESES ON MICROFICHE

I.S.B.N.

THESES CANADIENNES SUR MICROFICHE

National Library of Canada
Collections Development Branch

Canadian Theses on
Microfiche Service

Ottawa, Canada
K1A 0N4

Bibliothèque nationale du Canada
Direction du développement des collections

Service des thèses canadiennes
sur microfiche

NOTICE

The quality of this microfiche is heavily dependent upon the quality of the original thesis submitted for microfilming. Every effort has been made to ensure the highest quality of reproduction possible.

If pages are missing, contact the university which granted the degree.

Some pages may have indistinct print especially if the original pages were typed with a poor typewriter ribbon or if the university sent us a poor photocopy.

Previously copyrighted materials (journal articles, published tests, etc.) are not filmed.

Reproduction in full or in part of this film is governed by the Canadian Copyright Act, R.S.C. 1970, c. C-30. Please read the authorization forms which accompany this thesis.

THIS DISSERTATION
HAS BEEN MICROFILMED
EXACTLY AS RECEIVED

AVIS

La qualité de cette microfiche dépend grandement de la qualité de la thèse soumise au microfilmage. Nous avons tout fait pour assurer une qualité supérieure de reproduction.

S'il manque des pages, veuillez communiquer avec l'université qui a conféré le grade.

La qualité d'impression de certaines pages peut laisser à désirer, surtout si les pages originales ont été dactylographiées à l'aide d'un ruban usé ou si l'université nous a fait parvenir une photocopie de mauvaise qualité.

Les documents qui font déjà l'objet d'un droit d'auteur (articles de revue, examens publiés, etc.) ne sont pas microfilmés.

La reproduction, même partielle, de ce microfilm est soumise à la Loi canadienne sur le droit d'auteur, SRC 1970, c. C-30. Veuillez prendre connaissance des formules d'autorisation qui accompagnent cette thèse.

LA THÈSE A ÉTÉ
MICROFILMÉE TELLE QUE
NOUS L'AVONS REÇUE

NL-339 (r. 82/08)

Canada

LIFETIME MEASUREMENTS OF SOME S AND D STATES OF Cs I

by

© WILLIAM S. NEIL

A Thesis
Submitted to the Faculty of Graduate Studies through the
Department of Physics in Partial Fulfillment
of the Requirements for the Degree of
Master of Science at the
University of Windsor

Windsor, Ontario

1982

ABSTRACT

The natural radiative lifetimes of the nd $^2D_{5/2}$, nd $^2D_{3/2}$ (n = 7 to 14) and ns $^2S_{1/2}$ (n = 9 to 15) energy levels of atomic caesium have been measured. The time resolved fluorescence decay signal following pulsed laser excitation was analysed by an exponential-fitting computer program in order to extract a decay constant equivalent to the lifetime of the level being selectively excited. The measurements were performed at sufficiently low vapour densities to ensure that collisional effects were negligible.

Results of experimental work on the principal series line strength ratios of caesium have shown increasingly larger ratios than the expected ratio of statistical weights for configurations of higher principal quantum number. Some theoretical work suggests that the experimental findings can be attributed to spin-orbit configuration mixing which may occur in the heavy alkalis due to their strong spin-orbit interaction. This effect can also manifest itself by a difference in lifetimes of levels within a configuration although virtually no experimental work can be found attempting to measure these expectedly small lifetime differences especially for levels of higher energy and angular momenta.

The results of this experiment show that, for the levels measured, the intraconfiguration lifetimes differ by less than about 3 percent.

ACKNOWLEDGEMENTS

I would like to thank my supervisor, Dr. J.B. Atkinson, for his support and advice throughout the research. I would also like to express my appreciation to Mr. R. Niefer for his instruction on the laser systems used and many informative discussions in general.

Acknowledgements are due to Mr. R. Campbell and Mr. A. Ditchburn for work on the fluorescence cell and vacuum system glassware, to Mr. B. Masse for his work on the electronics systems and Mr. W. Grewe and his associates for their construction of some of the apparatus.

TABLE OF CONTENTS

LIST OF TABLES

LIST OF FIGURES

I. INTRODUCTION

Alkali metals are often used in experimentation because of their similarity to the atomic system of hydrogen. Theoretical models of hydrogenic systems are the most simple and thus can be more easily used to interpret experimental results. Caesium (Cs) being the heaviest of the available alkali metals has the largest spin-orbit interaction due to its large number of core electrons (54) and hence is of considerable interest because of the Fermi effect[1,2]. This effect is due to a large spin-orbit interaction which causes configuration mixing[3]. One effect of this mixing is to change the relative oscillator strengths for transitions between pairs of fine structure levels from the values given by the Ornstein-Burger-Dorgelo sum rule.

Experimental results[4] for the principal series of Cs have shown that oscillator strength ratios for the fine-structure doublets of higher principal quantum number are increasingly greater than the expected 2 to 1 ratio of $f_{3/2}$ to $f_{1/2}$. Other results[5] give a deviation of approximately 3 percent between the measured line strength ratios of the Cs 15d $^2D_{5/2}$ and 15d $^2D_{3/2}$ two-photon transitions to the 6s $^2S_{1/2}$ ground state and theory which neglects spin-orbit configuration mixing, although the error in the measurement was relatively large ($\pm$3 percent). Various theoretical calculations have been made [6,7,8,9] which take the spin-orbit effect into account although most of these are limited to the principal series of the alkalis. There is some disagreement within these results as to where a maximum in the oscillator strength ratio for the series may occur

and also with experimental results concerning the magnitude of the ratio, especially for levels of higher principal quantum number.

Configuration mixing can also manifest itself by a difference in the lifetime (τ) of levels within a given configuration because of their relationship with the line strengths. Using Warner's[6] theoretical oscillator strengths, the inverse lifetime ratio $A_{5/2}$ to $A_{3/2}$ for the 8d configuration of Cs is approximately 1.14 (see Appendix 1) although no measurements of both lifetimes have been found for comparison. Experimental results have been obtained with rubidium (Rb)[10,11] for the levels 4d $^2D_{5/2}$ and 4d $^2D_{3/2}$ which may be evidence of this effect. These measurements gave a 7 percent and 9 percent difference between the lifetimes of this fine structure pair, with each measurement having an error of about $\pm$7 percent. No lifetime measurements have been found which attempt to determine the effect of configuration mixing on the heavy alkali Rydberg levels where it is thought to be the most pronounced[2]. Measurements have been done for a series of nd ^2D_J level lifetimes for both Rb[10] and Cs[12,13] involving either fine structure level, J = 5/2 or J = 3/2, but not both. One experimental group[14] has published both 7d $^2D_{5/2}$ and 7d $^2D_{3/2}$ level lifetimes of Cs and although the initial results showed them as being different subsequent results[15] brought the lifetimes into agreement.

Pendrill[16] has measured the collisionally induced sensitized emission of fine structure levels of Cs after excitation of one of the levels in each nd ^2D_J pair for n = 9 to 14.

From his analysis of the two collisionally produced exponential decay components extrapolated to zero vapour density, it was concluded that the fine structure nd ^2D_J level pairs had equal free-atom lifetimes. Unfortunately, no estimate of the accuracy of the zero density intercepts was given although it was stated that the extrapolated values "appeared to converge (within large error bars) to plausible zero-density values". Upon observing one of the extrapolated sets of data in the above article, it is considered that the free-atom lifetimes have an error of about ± 5 to ± 10 percent which may be large relative to the differences that might exist between the lifetimes. The disadvantage of this method is that, as the vapour density is reduced, the sensitized fluorescence signal becomes much weaker than that obtained when measuring a direct transition from the level being excited, as in this experiment.

It is, therefore, apparent upon surveying available experimental results that there is little if any conclusive evidence of lifetime differences existing between the levels of any fine structure pair of the alkalis, or the magnitude of such differences if they indeed exist. Measurements are required for more and higher lying energy levels in order to resolve the effect of spin-orbit perturbation on intra-configuration lifetimes. In order to be able to measure natural or free-atom radiative lifetimes of levels and the small differences between them when within a configuration, it is necessary to consider other effects which may

influence the values of the measured lifetimes. The significant effects on which the lifetimes measured in this experiment may depend are collisional processes, diffusion effects and quantum beats.

A. Collisions

The quenching and mixing processes for the Cs D levels depicted in the reaction equations below can cause effective or measured lifetime to be much shorter than the natural lifetime and can cause multiple exponential components to appear in the fluorescence time decay when, in the absence of collisions, only one exponential component would be present. Quenching and mixing are due to inelastic collisions between excited atoms and other atomic or molecular species. These collisions result in an exchange of electronic and translational energy for atom-atom collisions with the addition of vibrational and rotational energy if molecular species are involved. When excited atoms are quenched, their population is reduced non-radiatively with time thereby allowing fewer radiative transitions from that level and a consequent change in the fluorescence decay intensity and time dependence which reduces the measured radiative lifetime. Mixing also causes non-radiative re-population of the initially excited level which results in additional decay components.

MIXING: $Cs(nd\ ^2D_{3/2}) + X \rightleftarrows Cs^*(nd\ ^2D_{5/2}) + X^*$ (1)

QUENCHING: $Cs(nd\ ^2D_J) + X \rightarrow Cs^*(\ ) + X^*$ (2)

In general, X can represent a ground state Cs atom or some foreign gas whether it be atomic or molecular in nature. Starred quantities represent atoms or molecules that have a different energy content from their unstarred counterpart as a result of a transfer of energy during a collision. The energy may be transferred between any of the translational, electronic, vibrational or rotational energies of the colliding species. $Cs^*()$ represents a caesium atom in any allowed energy level other than the one prior to collision or the other member level of its fine structure pair.

Pendrill[16] has shown that for collisions between excited and ground state Cs atoms the dominant effect is the transfer of population to the level energetically nearest the initially excited state. In the case of Cs nd ^2D_J levels it is the other member of the fine structure pair and for ns $^2S_{1/2}$ levels it is the (n-4)f ^2F_J levels. Since the fine structure levels within each pair are energetically very close to one another and it has been found[16] that the cross section for collisional transfer of population between two levels increases with decreasing energy defect, the dominant collisional process will be mixing while the transfer of population to all other levels, or quenching, will be relatively small.

If no contaminant gas is present and the Cs vapour density is sufficiently reduced so that collisional mixing is negligible, the fluorescence time decay signal from a level selectively excited in a fine structure level pair will consist of one decay component. The effective radiative lifetime obtained from this signal will be, neglecting other non-collisional effects, equivalent to the natural radiative lifetime of the excited level, within experimental error.

B. Diffusion

The trapping[17] or diffusion of fluorescence radiation is an effect of considerable importance when there are transitions to the ground state from the excited level that is being analysed for its lifetime. The population of an excited level is trapped when its fluorescent emission is re-absorbed before escaping from the region of the vapour that is being observed, thus effectively extending its measured radiative lifetime. In order for re-absorption to occur, the levels to which transitions from the excited level are being made must have an appreciable population. In appendix 2, calculations are performed which show that the lowest P level to ground state transition was trapped by only a small amount under the conditions at which the experiment was performed. Since the population induced into any of the S and D levels was much less than that of the ground state and was distributed among all of the energetically lower levels to which

transitions were allowed, the effect of trapping on the measured lifetimes of the S and D levels should be negligible.

Another diffusion effect is the diffusion of excited atoms out of the region of observation in the fluorescence cell. Excited atoms leaving the region of observation before radiating allows a loss mechanism for the excited state population that is being observed other than by radiation. This effect can change the fluorescent decay time dependence and effectively cause the measured radiative lifetime to be shorter than the natural lifetime. Under the low vapour density conditions of this experiment, the Cs atom mean free path was much larger than the observation region so that atoms would freely migrate rather than diffuse out of the region of observation with time. The distance the excited atoms could travel during a typical length of time that the time resolved signal would be collected following each laser pulse and the size of the excitation region relative to the observation region size were such that thermal distortion of the measured lifetimes due to thermal migration was negligible (see appendix 3).

C. Quantum Beats

A topic of recent interest and another effect that can alter the time dependence of the fluorescence decay signal is the presence of quantum beats[18,19]. Single atom quantum beats result from pulsed coherent polarized excitation to a superposition of hyperfine[20] sub-levels for each ns $^2S_{1/2}$ or nd ^2D_J level. The fluorescent

time decay signal contains modulation at frequencies corresponding to the energy separations of these sub-levels. The quantum beat signal is polarization sensitive both in excitation and subsequent decay and therefore can be suppressed by the proper choice of angle between the excitation polarization and detection polarization thereby, ideally, eliminating this effect on the measured lifetimes.

It is hoped that the results from this experiment not only verify previously measured lifetimes but, also, that these and the previously unmeasured lifetimes allow a better understanding of the effect of spin-orbit configuration mixing on the fine structure levels of the heavy alkali atoms.

II. THEORY

When energy is imparted to an atom so that one or more of its electrons are raised from the ground to an excited state i, it may radiatively relax or become de-excited to an energetically lower state j at a rate A_{ij} which is a constant for a given transition. A_{ij} is the Einstein coefficient for spontaneous emission for the transition i → j and $A_{ij}^{-1} = \tau_{ij}$ is the natural radiative lifetime of the TRANSITION. If transitions to more than one level j are allowed from the excited state then

$$\sum_j A_{ij} = A_i = \tau_i^{-1} \quad , \tag{3}$$

where τ_i is the natural radiative lifetime of the LEVEL i since each of the A_{ij} coefficients contribute to the overall relaxation of the excited level.

If $N_i(t)$ is the population density of the level i at the time t, then its spontaneous decay rate is given by

$$\frac{dN_i(t)}{dt} = -A_i N_i \quad . \tag{4}$$

The solution of this differential equation is:

$$N_i(t) = N_i\ (t = 0)\ e^{-A_i t} \quad , \tag{5}$$

which shows that the population in the excited level will decay exponentially from the time of its initial population at t = 0 with

a decay constant A_i. Since the time evolution of the radiative signal observed resulting from any allowed transition from the excited level depends on the population of that level at any time, this signal will decay exponentially in time with a decay constant equal to the lifetime of the excited level.

The above discussion does not consider transition rates into or out of the excited level due to collisions or radiative cascading from energetically higher levels. Since equation (4) is valid only for the case of free atoms it must be modified to take into account the collisional processes which occur within a vapour. Since the transitions observed were from selectively excited levels, radiative cascading from higher levels should not be a problem.

Although many different collisionally induced transitions can in principle occur, it has been found[16] that the dominant process after a level is selectively excited is collisional mixing with the energetically nearest level. The rate equations for a pair of collisionally mixed levels 1 and 2 are:

$$\frac{dN_1}{dt} = -A_1N_1 - Z_{12}N_1 + Z_{21}N_2 \quad , \qquad (6)$$

and

$$\frac{dN_2}{dt} = -A_2N_2 - Z_{21}N_2 + Z_{12}N_1 \quad . \qquad (7)$$

The Z_{ij}'s are collision numbers which represent the average number of collisions per atom per unit time that are effective in causing an electronic transition from level i to level j. The collision number can be written in terms of an effective cross section for the collisionally induced transition as:

$$Z_{ij} = NQ_{ij}\,\bar{V}_r \quad , \tag{8}$$

where N is the atomic ground state density of Cs and

$$\bar{V}_r = \left(\frac{8kT}{\mu\pi}\right)^{\frac{1}{2}} \tag{9}$$

is the mean relative velocity of the collision partners which is written in terms of the reduced mass μ, Boltzmann's constant k and the absolute temperature T. The relationship between Z_{12} and Z_{21} given by the principle of detailed balancing is

$$\frac{Z_{12}}{Z_{21}} = \frac{g_2}{g_1}\, e^{(E_1 - E_2)/kT} \quad , \tag{10}$$

where g_1, E_1 and g_2, E_2 are the statistical weights and energies of levels 1 and 2 respectively and k is Boltzmann's constant. The exponential term represents the fraction of collisions that involve a relative kinetic energy greater than the energy separation of levels 1 and 2.

The dominant collisional process being mixing between

energetically nearest levels is intuitively reasonable as far as collisional cross sections are concerned when Franck's rule[16] and equation (10) are considered. According to Franck's empirical rule, as the separation between energy levels increases, the collisional transfer cross section is reduced so that collisional effects should dominate between energetically close levels, neglecting the population of the levels. Also, for large energy level separations the exponential term in equation (10) causes one of the cross sections between two collisionally coupled levels to dominate. At small energy separations the exponential term is approximately unity causing the collision cross section ratio between the levels to be essentially the ratio of their statistical weights so that small energy separations are more conducive to collisional mixing.

For selective excitation of nd ^2D_J or ns $^2S_{1/2}$ levels as in this experiment, collisional mixing will occur between nd $^2D_{3/2}$ and nd $^2D_{5/2}$ or ns $^2S_{1/2}$ and (n - 4)f ^2F_J levels respectively since these are energetically closest. (See Fig. 1 for 8d ^2D_J and 10s $^2S_{1/2}$ levels.) The energy separation of the nd ^2D_J fine structure levels, E(nd $^2D_{5/2}$) - E(nd $^2D_{3/2}$), is small relative to kT under the conditions of the experiment so that the ratio of collision cross sections between the levels of each nd ^2D_J fine structure pair given by (10) is

$$\frac{Q_{3/2\rightarrow 5/2}}{Q_{5/2\rightarrow 3/2}} \approx \frac{6}{4} \qquad (11)$$

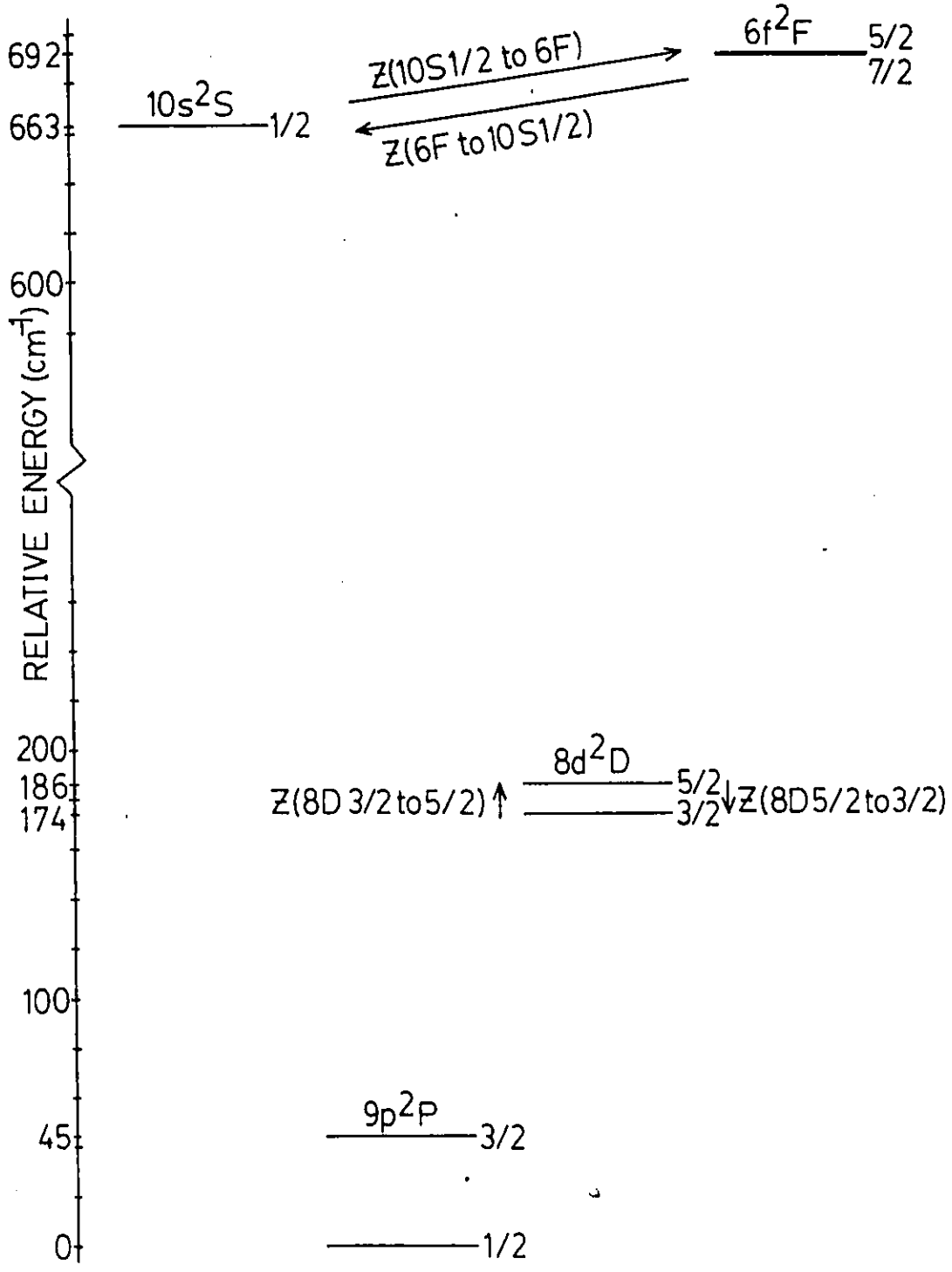

Fig. 1 Relative energy separations for neighbouring fine level pairs of Cs. The nd $^2D_{5/2}$, nd $^2D_{3/2}$ levels and the ns $^2S_{1/2}$, (n-4)f ^2F levels are the most strongly collisionally coupled when selective excitation is to an nd ^2D_J or ns $^2S_{1/2}$ level respectively. Arrows show directions of collisional population transfer.

The ns $^2S_{1/2}$ and (n - 4)f ^2F level mixing will not be considered since the energy separation between these levels is larger than for the levels of a nd ^2D_J fine structure pair of comparable energy.

The system of two coupled rate equations (6) and (7) has a general solution (for details see reference 16)

$$N_i(t) = X_{i(+)}e^{-\lambda_{(+)}t} + X_{i(-)}e^{-\lambda_{(-)}t} \quad , \qquad (12)$$

where i is 1 or 2 which represent the nd ^2D_J fine structure levels J = 3/2 and J = 5/2, and

$$\lambda_{(\pm)} = \frac{1}{2}(A_1+A_2) + \frac{1}{2}(Z_{12}+Z_{21}) \pm \frac{1}{2}\left[(A_1-A_2)^2 + 2(A_1-A_2)(Z_{12}-Z_{21}) + (Z_{12}+Z_{21})^2\right]^{\frac{1}{2}} \qquad (13)$$

The coefficients $X_{i(+)}$ and $X_{i(-)}$ depend on which of levels 1 and 2 is being selectively excited. Following excitation (at t = 0) of level 2, the population densities of levels 1 and 2 are $N_1(0) = 0$ and $N_2(0) = N^*$, and their time dependence will be given by

$$N_1(t) = \frac{N^*Z_{21}}{\lambda_{(-)}-\lambda_{(+)}}(e^{-\lambda_{(+)}t} - e^{-\lambda_{(-)}t}) \quad , \qquad (14a)$$

and

$$N_2(t) = \frac{N^*}{\lambda_{(-)}-\lambda_{(+)}} \left\{ \left[\lambda_{(-)} - (A_2+Z_{21}) \right] e^{-\lambda_{(+)} t} + \left[(A_2+Z_{21}) - \right.\right.$$

$$\left.\left. -\lambda_{(+)} \right] e^{-\lambda_{(-)} t} \right\} \qquad (14b)$$

The results obtained from the above theory which considers only collisional mixing of the selectively excited level with the energetically closest level, gives just two density dependent exponential decay components $\lambda_{(\pm)}$ in the time evolution of the excited state population density. According to this theory, as the Cs vapour density N is reduced, the decay components $\lambda_{(+)}$ and $\lambda_{(-)}$ of the fluorescence signal will change as in figures 2(a) and (b) depending on whether the natural lifetimes of the collisionally mixed levels are the same or not. The amplitude ratio $X_{(+)}/X_{(-)}$ for the decay components in transitions out of the selectively excited level is:

g_1/g_2 ; $N_2(0) = N^*$, for $A_1 = A_2$ and all $N\bar{V}_r$

g_2/g_1 ; $N_1(0) = N^*$, for $A_1 = A_2$ and all $N\bar{V}_r$

g_1/g_2 ; $N_2(0) = N^*$, for $A_1 \neq A_2$ and in the limit of $N\bar{V}_r \to \infty$

g_2/g_1 ; $N_1(0) = N^*$, for $A_1 \neq A_2$ and in the limit of $N\bar{V}_r \to \infty$

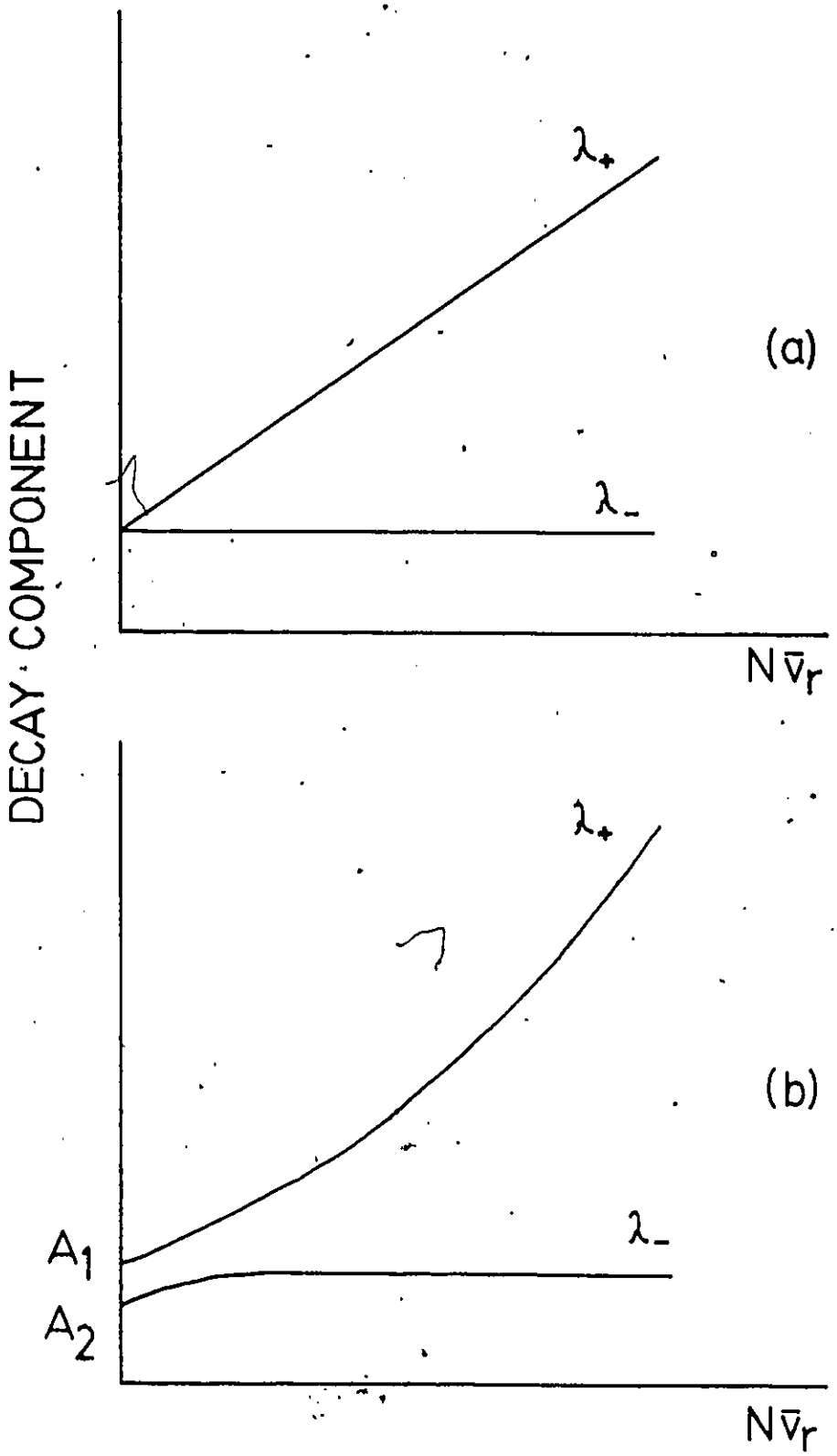

Fig. 2 Collisional decay component dependence on $N\bar{v}_r$ for (a) $A_1 = A_2$ and (b) $A_1 \neq A_2$.

0 ; $N_2(0) = N^*$, for $A_1 \neq A_2$ and in the limit of $N\bar{V}_r \to 0$

∞ ; $N_1(0) = N^*$, for $A_1 \neq A_2$ and in the limit of $N\bar{V}_r \to 0$

In any case, the natural radiative lifetime of a level selectively excited can be measured within experimental error by causing the atomic vapour density to be sufficiently low. Calculations using the collisional mixing theory discussed above and the collision cross sections of Deech et al.[12], which show that the Cs vapour density used in this experiment allows essentially non-collisionally perturbed radiative lifetimes to be measured are in appendix 4.

III. METHOD OF LIFETIME DETERMINATION

Various methods have been used to determine the lifetimes of atomic energy levels using both direct and indirect means.[25,26] The method used in any particular experiment will depend upon various factors such as the length of lifetime and size of atom to be studied or the excitation energy required and will determine the methods of excitation, signal collection and lifetime retrieval necessary to obtain satisfactory results.

A direct method of lifetime determination, and the one used in this experiment, involves time resolution of fluorescence.[27] In particular, a two stage pulsed Nd:YAG laser was used to pump a two stage tunable wavelength dye laser which selectively excited individual atomic fine structure levels using two-photon non-resonant pumping, as shown in the energy level diagram of figure 3. The subsequent fluorescence signal in the strongest transition from the excited level was collected in a time resolved digitized fashion following each laser pulse after wavelength discrimination using a grating monochromator. Under certain conditions, this signal can be computer program fitted to a single exponential decay constant A which gives directly the natural lifetime $\tau = A^{-1}$ of the selectively excited level. Since this experiment requires the excitation of relatively highly lying energy levels, of the same parity as the ground state and whose relative energy separations and lifetime differences are small, the methods of excitation and signal collection which were used were considered to be the most attractive for the reasons presently discussed.

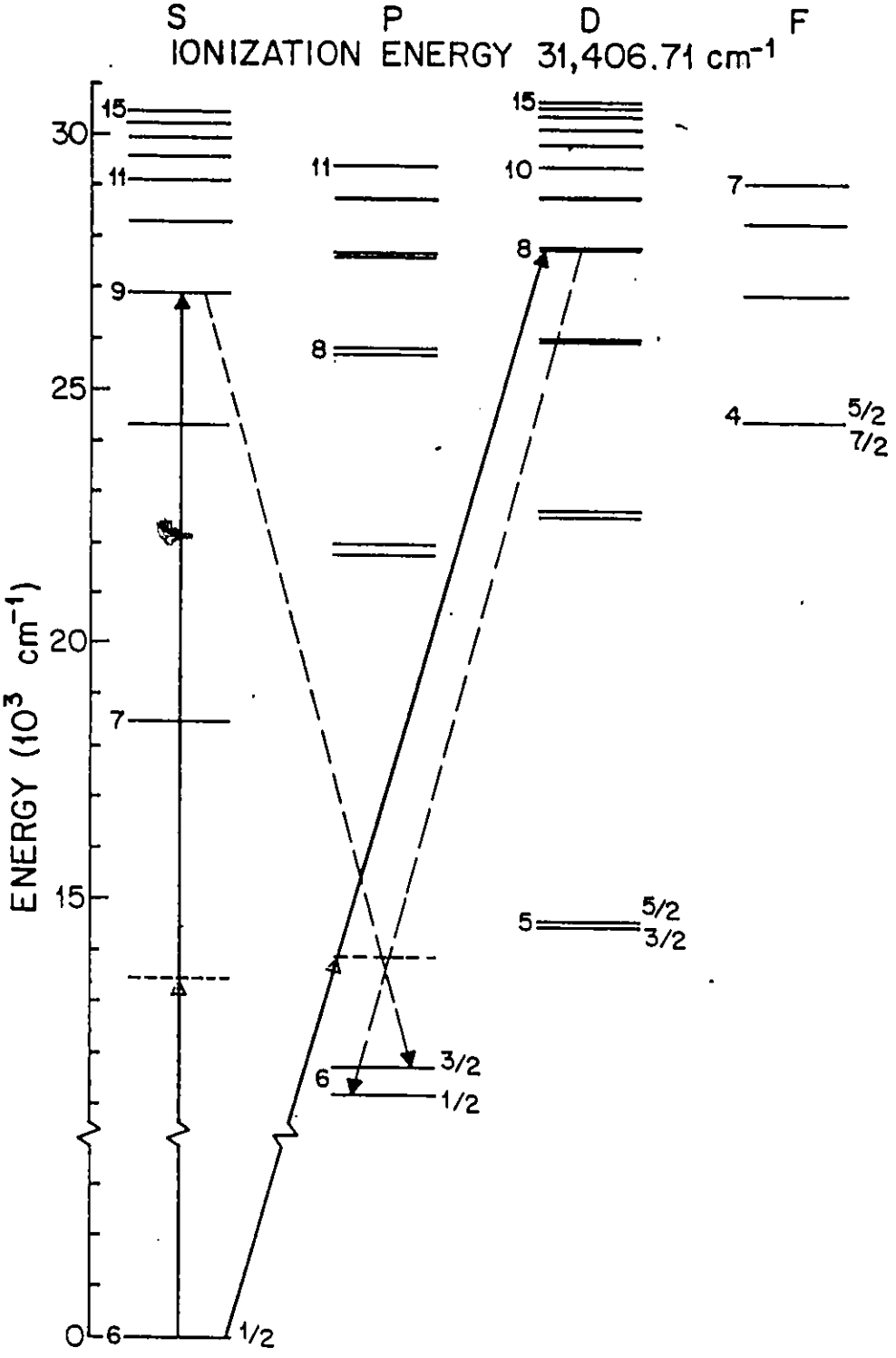

Fig. 3 Cs I energy level diagram showing typical selective excitation and observed resultant fluorescence. Solid arrows represent selective two-photon laser excitation via an intermediate (dashed) virtual level. Dashed arrows represent the transitions observed in fluorescence. The numbers to the immediate left of the energy levels are the principal quantum numbers n, to the immediate right are the total angular momentum quantum numbers J.

The levels whose lifetimes are under study (L = 0 and 2) are not connected to the ground level (L = 0) by allowed single photon dipole transitions ($\Delta L = \pm 1$). It is necessary therefore, to use either a single photon quadrupole transition[11] ($\Delta L = 0, \pm 2$) or a two-photon dipole transition[28] ($\Delta L = 0, \pm 2$) as a direct method of excitation. It should be noted that cascade fluorescence spectroscopy[29] can be used although this method has the disadvantage of indirectly exciting the level under investigation causing further complications in lifetime analysis. Quadrupole transitions, typically, have a relatively small absorption probability while the two-photon process depends on the degree to which the first photon absorption is resonant in energy with intermediate states (see figure 4). Excitation using two photons of the same wavelength, as is used in this experiment, is normally non-resonant thus decreasing the absorption probability, although, for the levels excited in this experiment, nearby intermediate energy levels exist allowing reasonable absorption. For this reason and the fact that this method of excitation does not complicate the excitation source, as does step-wise excitation which uses two resonant photons of different wavelengths, it was chosen as the method of excitation. Regardless of which type of two-photon excitation is being used, a pulsed laser is necessary in order to selectively induce a large enough excited state population for the fluorescence to be observable and for excitation times to be short so that the free atom radiative decay can be measured.

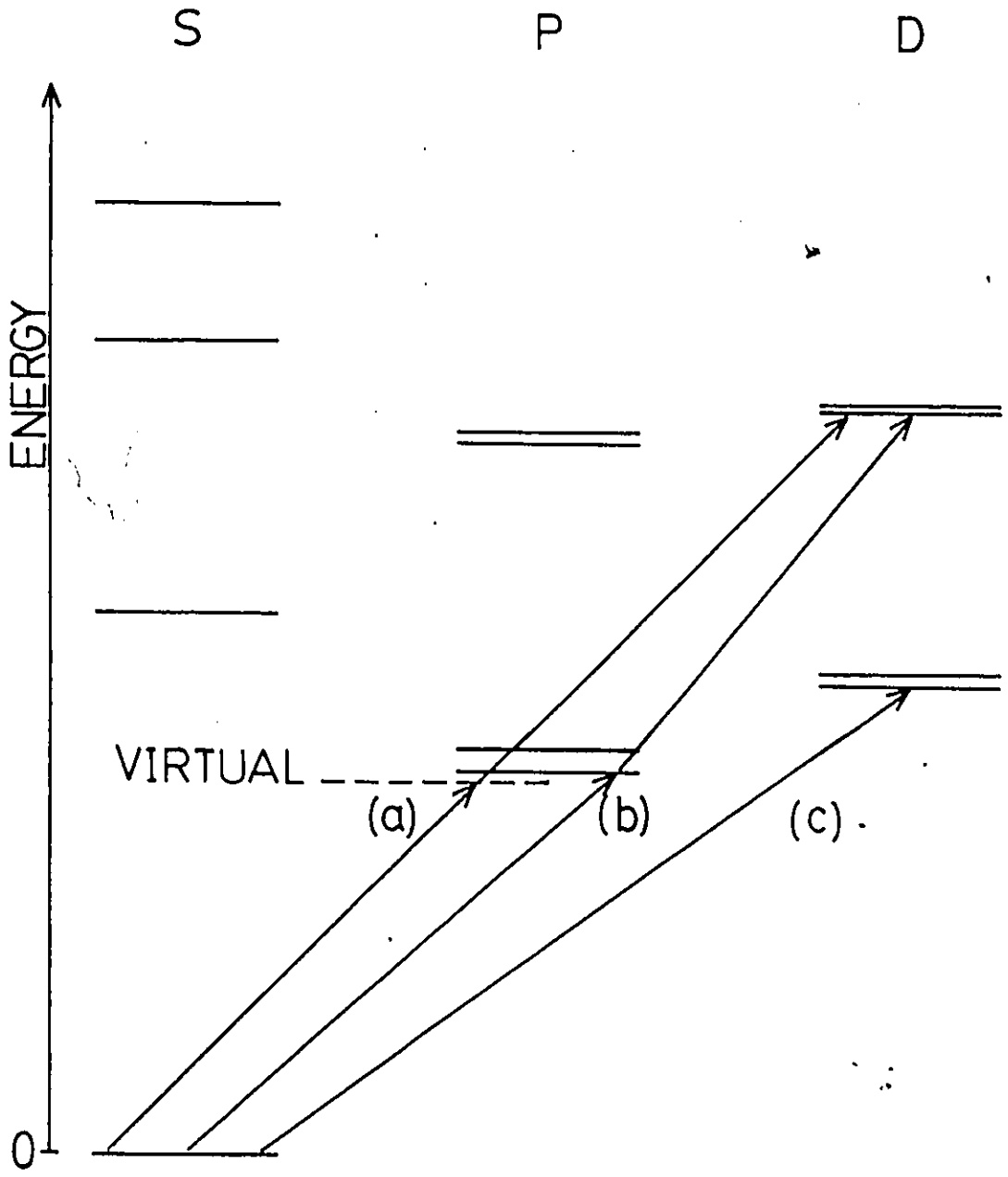

Fig. 4 A few methods of excitation used to populate D levels. (a) Non-resonant two-photon excitation, (b) step-wise or resonant two-photon excitation and (c) single photon quadrupole excitation. All of these methods reach a final level not achievable by single photon dipole transitions. As excitation proceeds to higher energy levels the wavelengths for (c), which are about twice as short as for the other two processes, will make this method of excitation less attractive since it is difficult to generate sufficient dye laser output intensities in the shorter wavelength spectral region because of the inefficiency of laser dyes.

A further advantage of two-photon excitation for high energy levels is that it allows the dye laser system to operate in a more efficient dye spectral range since the wavelengths used are twice as long as those used in single photon absorption so that the dye range will be shifted from the less efficient ultraviolet region toward the more efficient red end of the optical spectrum. The non-resonant intermediate state excitation has the additional advantage of allowing the fluorescence signal to be more easily separated from laser scatter before detection since they are of different wavelengths.

Since the levels being selectively excited are of relatively high principal quantum number n, and the number of levels to which an excited level can radiate increases with n, the magnitude of the branching ratios for transitions from an excited level of principal quantum number n decreases as n increases. This causes a reduction in the amount of fluorescence signal that is available in any one transition. In order to collect enough signal to have acceptable counting statistics over a length of time at least as great as four times the lifetime being measured, and to do this in a reasonable period of time, the signal collection efficiency must be high. To be able to separate transitions from closely spaced energy levels it is also necessary to have a relatively narrow detection bandwidth which, unfortunately, is at the expense of the total signal which reaches the signal collector. In the method of signal collection used, essentially all fluorescence

signal detected by the photomultiplier after wavelength discrimination is collected following each laser pulse for a predetermined length of time. This is done with a minimum time resolution of approximately 0.02τ using a transient digitizer/recorder.

IV. DESCRIPTION OF APPARATUS

The apparatus basically consisted of a Nd:YAG pumped tunable dye laser, a fluorescence cell in a heated oven, a spectrometer consisting of a monochromator, photomultiplier and photomultiplier pulse amplifier, a transient waveform digitizer/recorder and a microcomputer. A block diagram of the apparatus is shown in figure 5.

A. The Laser System

The excitation source for the dye laser was a Quanta-Ray Nd:YAG laser model DCR-1A with an output wavelength of 1064 nm which was rated at 700 mJ maximum output with a 10 ns pulse length. This laser was equipped with special optics in order to give a more uniform energy distribution over the cross section of the output beam. This output was then frequency doubled to 532 nm using a Quanta-Ray harmonic generator in which an angle tuned KD^*P crystal was used. The doubling efficiency was approximately 30 percent at 2/3 rated output. The linearly polarized second harmonic was spatially separated from the unconverted fundamental wavelength using a Pellin-Broca prism which completely separated the two beams over a distance of about 35 cm. The second harmonic beam was then directed 90 degrees from its original path by a CVI 45 degree high power laser mirror coated for 532 nm into a homemade two stage dye laser (see figure 6). The fundamental was directed into a beam stop which reduced the hazards of scattered infrared radiation.

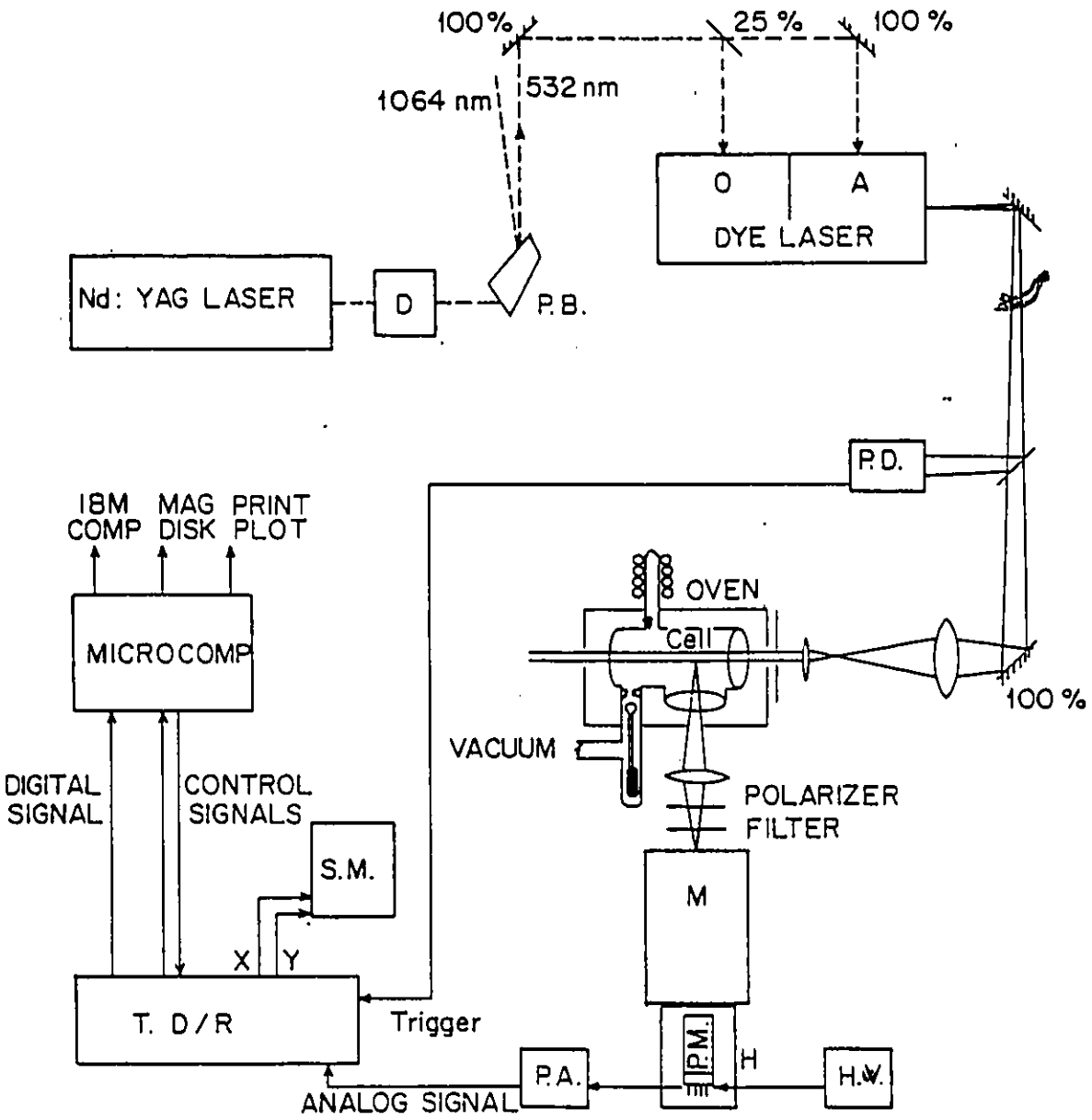

Fig. 5 Apparatus block diagram

A - dye laser amplifier stage
D - crystal frequency doubler
H - Peltier P.M. cooling unit and housing
H.V. - P.M. high voltage supply
M - monochromator
O - dye laser oscillator stage
P.A. - P.M. pulse amplifier
P.B. - Pellin-Broca prism harmonic separator
P.D. - photodiode detector
P.M. - photomultiplier tube
S.M. - C.R.T. signal monitor
T.D/R - transient digitizer/recorder.

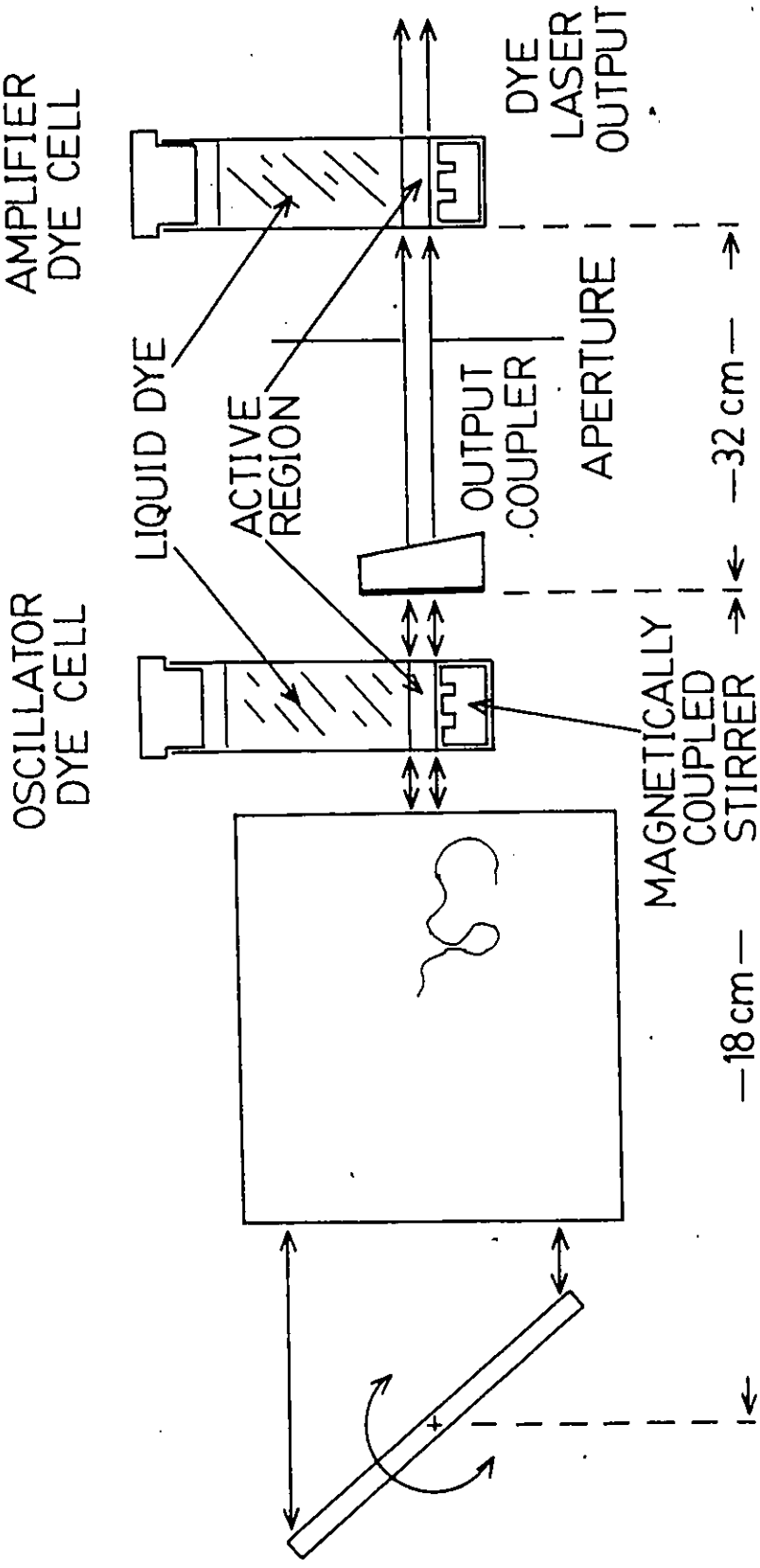

Fig. 6 A two stage dye laser with dye cells transversely pumped by the Nd:YAG's 532 nm second harmonic.

Two 45-degree mirrors of 25 and 100 percent reflectivities, coated for 532 nm, coupled the second harmonic beam into the oscillator and amplifier stages of the dye laser respectively. The beams reflected into both stages were then focused into each dye cell using cylindrical quartz lenses of 5 cm diameter. The size of the excited volume in the liquid dye was about 2 mm in height, less than 1 mm in depth and in length was the inside width of the dye cell or about 8 mm. The dye cells were a fixed volume type, model 509 made by Precision Cells Inc., and were magnetically stirred. The amount of liquid dye used in each cell was approximately 2 cm^3 and lasted from 15 minutes to 6 hours, operating at 10 pps and about 100 mJ of 532 nm excitation energy per pulse, depending on the dye used before photodegradation caused a serious decrease in dye laser output power. The dyes used were DOTC, OXAZINE 725, OXAZINE 720, DCM and a RHODAMINE 640 - CRESYL VIOLET PERCHLORATE mixture which were purchased from the Exciton Corporation. Together, the dyes covered a lasing range from 651 nm to 767 nm allowing two-photon excitation of the levels 7d ^2D_J to 15d ^2D_J of Cs. The dye laser output power was a maximum at oscillator dye concentrations in the range of $2x10^{-3}$ to $5x10^{-4}$ moles per litre using ethanol or methanol as solvent and with a reduced concentration, by a factor of two, for the amplifier stage. The output energy was measured using a Scientech 362 power/energy meter with a surface type detector. The range of dye laser powers used was measured to be from 0.8 to 2.5 mJ per

pulse giving a dye laser efficiency of about 3 percent.

The wavelength tuning mechanism in the dye laser oscillator stage was a Bausch and Lomb 52 mm square diffraction grating with a groove density of 600 per mm and a 54 degree blaze angle. The specified efficiency was 54 percent in the fourth order at 643.8 nm. During the experiment the grating was used in fourth order from 51 to 67 degree angle of incidence in the wavelength range stated above. The grating was used in a Littrow configuration in conjunction with a homemade x28 quad-prism beam expander. The beam expander was used to maximize the grating resolution by spatially expanding the dye fluorescence in one dimension in order to cover the full ruled width of the grating near the largest incidence angle used. The grating assembly could be rotated about an axis perpendicular to both the optical axis of the laser and the direction of expansion by the beam expander, but parallel to the grating grooves. The micrometer screw adjustment on the grating assembly caused a change of about 1.3 cm^{-1} in dye laser spectral output per smallest scale division on the micrometer calibration. This corresponds to an adjustment of about one-half of a smallest scale division from the 14d $^2D_{3/2}$ to the 14d $^2D_{5/2}$ level since the excitation is a two-photon process which effectively doubles the change in laser output wavelength.

The direction of linear polarization of the second harmonic pump beam used to excite the dye laser was perpendicular to the grating grooves. This allowed greater reflection efficiencies from the beam directing mirrors, a higher diffraction efficiency from the dye laser grating and a higher transmission through the quad-prism beam expander.

The oscillator output was coupled into the amplifier stage by either a 10 percent or 40 percent broadband reflector depending on the conversion efficiency of the dye used. The oscillator cavity length, the distance between the output coupler to the centre of the grating, was measured to be about 18 cm corresponding to a separation between cavity modes of about 0.83 GHz or 0.028 cm^{-1}. The spectral width of the dye laser output was estimated to be less than 0.3 cm^{-1} and contained a cavity mode structure. This was done by observing the fringe width of an interference pattern from a Quanta-Ray broadband Fabry-Perot monitor etalon with a free spectral range of 1 cm^{-1} as can be seen in figure 7. The dye laser output half-angle of divergence was estimated by measuring the change in beam diameter over a distance of about 9 m and was found to be approximately 3 milliradians.

B. The Fluorescence Cell

The dye laser beam travelled a distance of about 9 m and was re-directed by two first surface uncoated aluminum mirrors before reaching the beam diameter reducing optics situated in front

Fig. 7 Reproduction of a photograph taken of a typical interference pattern from a Fabry-Perot monitor etalon with a free spectral range of 1 cm^{-1}. The cavity mode structure cannot be seen because of its frequency instability causing spatial movement of its interference fringes during the exposure time. The exposure was taken for a period of time equivalent to approximately 80 laser pulses.

of the fluorescence cell entrance window. The beam diameter was reduced from about 2.5 cm to about 2 mm by 2 lenses in a confocal arrangement. The diameter and focal lengths of the first and second lenses were 9 cm and 23 cm, and 1.8 cm and 2 cm respectively. The beam diameter was reduced rather than focused into the fluorescence cell since the region of detection was about 1 cm in length requiring a uniform photon flux density and the fluorescence detector entrance was a slit.

After being reduced in size the beam passed through the cell oven and cell entrance windows directly in front of and as close as possible to the observation window facing perpendicular to the beam path. Observing at right angles to the beam allowed the laser radiation and consequent fluorescence to be more easily separated while the effect of trapping, the diffusion of radiation, was minimized by making the separation between the laser beam and observation window as small as possible (see figure 8). The detection region began immediately after the beam entered the cell so that no excitation energy was absorbed causing fluorescent emission before the region of observation. This did not create a problem since both the vapour density and the absorption oscillator strengths were low, allowing the excitation depth into the Cs vapour to be large. The laser beam passed out of the cell through the cell exit window which was attached at a slight angle in order to reduce back-reflected light into the region of observation. In order to reduce scattered laser light, the oven's inner walls and

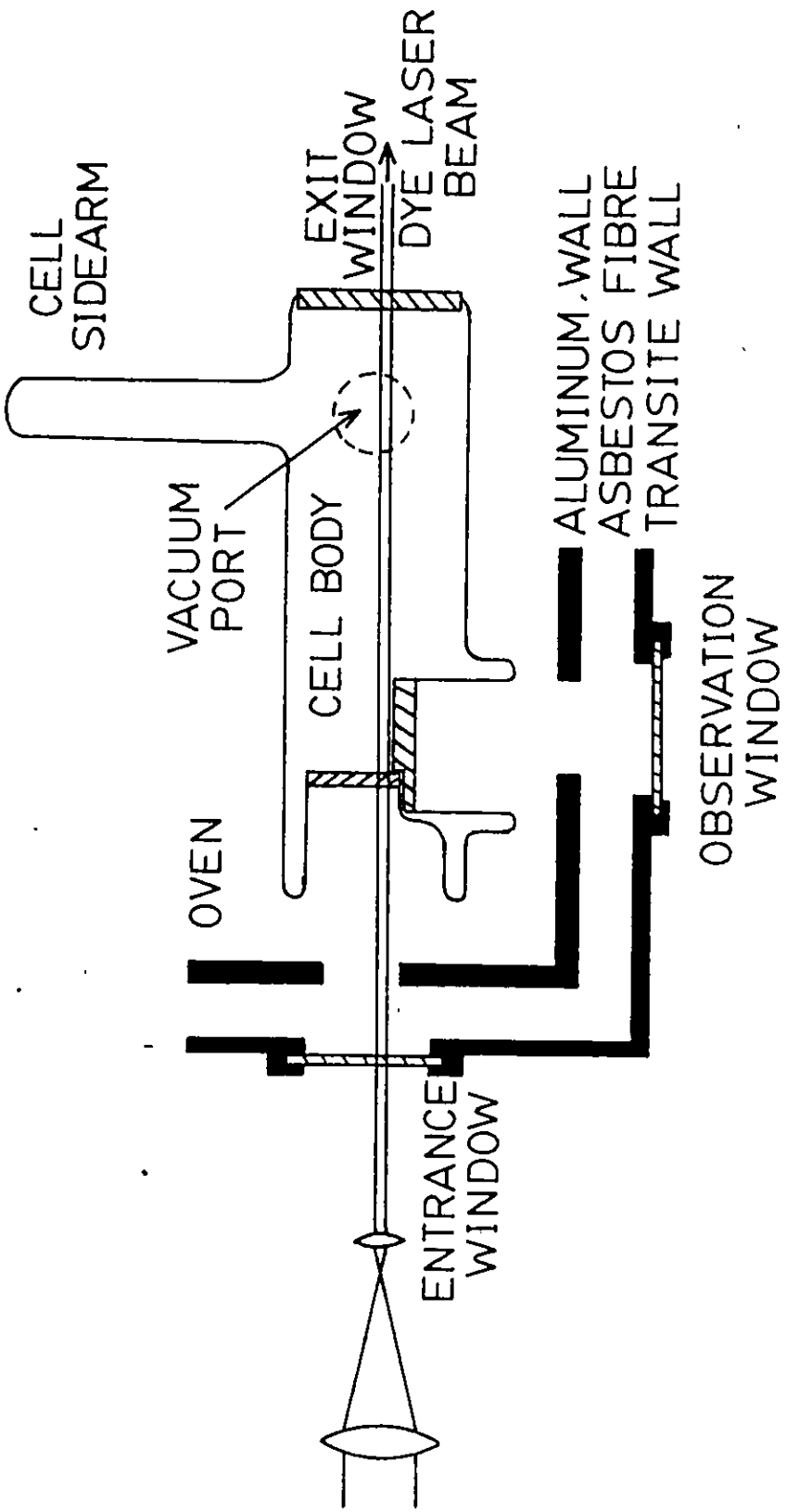

Fig. 8 Fluorescence cell arrangement (cross-section).

some outer surfaces of the fluorescence cell were coated with colloidal graphite. The fluorescence cell itself was made of 7740 pyrex glass, was cylindrical in shape, and had a diameter of 3.5 cm and a length of 11 cm.

The fluorescence cell was connected to a vacuum system with a base pressure of about 3×10^{-7} torr measured using a CVC gauge control unit type GIC-110C with a CVC ion tube type GIC-028-2 running at an emission current of 8.7 milliamperes. The ion tube was located next to the cell in order to reduce the effect of a pressure gradient which might have existed between the cell and vacuum pump. The pumping system consisted of an Edwards Speedivac single stage mechanical roughing pump model ISC 50B and an Edwards model E-02 diffusion pump. The cell and vacuum system were isolated from one another by a greaseless ground glass magnetically operated stopcock with a 2 mm bore. To achieve the above pressure, the vacuum system glassware, including the fluorescence cell, was baked while being evacuated at a minimum of 150°C, which was three times the normal operating temperature, for about one week. After baking, about one gram of pure natural Cs (obtained from Materials Limited of Fairfield, New Jersey) was distilled into the cell. The cell was contained within an oven which controlled the temperature of the Cs vapour in the cell body. The oven was double walled, the inner aluminum wall being thermally insulated from the outer transite wall by asbestos fibre. A resistance wire heating element running along the oven's inner walls carried a D.C. current of 0.72A which held the cell body temperature at about 55°C. Directly

attached to the cell body and extending out of the oven was a sidearm 8.6 cm in length with an inside diameter of 1.2 cm which served as a reservoir for the Cs. The sidearm temperature was controlled by a Tamson thermostatic oil circulator which circulated oil through a copper coil thermally coupled to the sidearm. The sidearm temperature of $28\pm1\,^{\circ}C$ was the lowest on the fluorescence cell surface and was used to control the density of Cs vapour in the cell body. The cell body temperature was kept at least $20\,^{\circ}C$ higher than the sidearm temperature to prevent Cs vapour from condensing on the entrance and observation windows. The temperatures were measured using copper-constantan thermocouples with an ice-water reference junction temperature. The junctions were kept in thermal contact with the pyrex cell by using a ceramic paste. The thermoelectrically induced voltages were measured using a Leeds and Northrup millivolt potentiometer which was used in conjunction with a Leeds and Northrup conversion table for thermocouples in order to convert the voltages to temperatures.

C. Detection and Collection System

The fluorescence produced by each laser excitation pulse was observed perpendicular to the direction of excitation in an observation half-angle of about 6.5 degrees. This was done by placing an aperature limited spherical lens, of 8.5 cm diameter and 9 cm focal length, 20.5 cm from the excitation region in the cell and 16 cm from the monochromator entrance slit (using the Gaussian lens

formula to calculate the distance). The laser beam was adjusted so that it would be parallel with the entrance slit. Before entering the monochromator the light from the fluorescence cell was made to pass through a Ditrics Optics short wavelength pass filter in order to decrease the amount of laser scatter in the cell from entering the detection system. This filter had a short wavelength average transmission of 70 percent and a long wavelength transmission of less than one percent. When only one component of polarization was to be detected, a polarizing film was also placed in the path of the fluorescence before the monochromator.

The Jarrell-Ash 0.25m f/3.5 Ebert monochromator was measured to have a full bandwidth resolution of about 6 nm at 600 nm using 1 mm entrance and exit slits. This estimation was made by detecting the 8d $^2D_{3/2}$ to 6p $^2P_{1/2}$ transition in Cs and observing at what wavelengths the signal decreased to a negligible amount on either side of the transition. The monochromator slit sizes used during the experiment were 1 mm or 0.5 mm depending on the required spectral resolution and length of lifetime being measured.

After passing the monochromator exit slit, the fluorescence signal was directed onto the photocathode of an RCA photomultiplier tube model C31034 by a 4 cm diameter, 4 cm focal length lens. The photomultiplier (PM), which had a specified and measured pulse rise time of 2.5 ns, had an essentially flat spectral response over the spectral range used in the experiment. The pulse amplitude measured on the 50 ohm input of a Tektronix 7844 oscilloscope using a 7B92A time base module was found to range from the 3 mV

noise level to nearly 50 mV. The PM tube was contained in a Pacific Photometric Instruments housing model 3457 which contained an air cooled thermo-electric cooling unit which used a model 33 temperature control unit. Operation of the PM tube at a reduced temperature caused it to have a lower dark current. The dark current pulse rate under normal operating conditions was found to be roughly 175 per second. The longest data accumulation scan of the signal recorder was about 4 μs in length and occurred at the laser repetition rate of 10 pps. The PM's duty cycle was then 4×10^{-5}. Since the signal pulse collection rate was typically 10 to 20 per second, the signal to noise ratio was normally better than 2000:1. In order to have a further reduction in background noise, the entire fluorescence detection system including filters, monochromator and photomultiplier were kept in an opaque enclosure connected directly to the fluorescence cell oven.

The PM tube output was connected by means of a 65 cm length of shielded 50 ohm coaxial cable to a 50 ohm shunt resistor at the 1000 ohm input of an Ortec Timing Filter Amplifier model 454. With the filter in the minimum time constant position, its specified pulse rise time was 4.5 ns. The output of the amplifier, which was set to invert the negative PM pulses was connected to the 50 ohm input of the Biomation Waveform Digitizer/Recorder model 6500 by a 32 cm length of shielded 50 ohm coaxial cable. This device digitized and stored in its memory the time resolved signal from the PM amplifier for a time equivalent to 1024 channels each of 2, 5 or 10 ns

duration depending on the length of the lifetime being measured. The Biomation began collecting the signal after receiving an "arm" pulse from a PET 2001 microcomputer and a "trigger" pulse from a photodiode located just before the fluorescence cell which detected each laser pulse. The photodiode used was an EG&G SGD-100A which had a measured rise time of 8 ns.

Each "scan" of the fluorescence signal was digitized and stored in the Biomation memory, an example of which is shown in figure 9. This data was then transferred under microcomputer control into the computer's memory before the next laser pulse. The computer was programmed to take the digital signal in each channel of a Biomation scan and add it to the corresponding channel of previously accumulated scans. When the summed digital signal amplitude in any channel reached a predetermined amount which ensured acceptable counting statistics over a sufficient length of a particular energy level's fluorescence decay, the accumulation was halted.

This method of data collection requires that any channel of one scan represent the same position in time following the laser pulse as the corresponding channel of any other scan. This was measured to be the case within ± 1 channel for the range of dye laser intensities incident on the photodiode detector that occurred throughout the experiment. The amplitude resolution of each digitized scan was 1 in 64. Since the input voltage range used was ± 250 mV the voltage resolution was about 8 mV. The PM amplifier gain was adjusted so that the smallest PM pulses were at least of 8 mV amplitude after amplification so that their digitized amplitude would be 1.

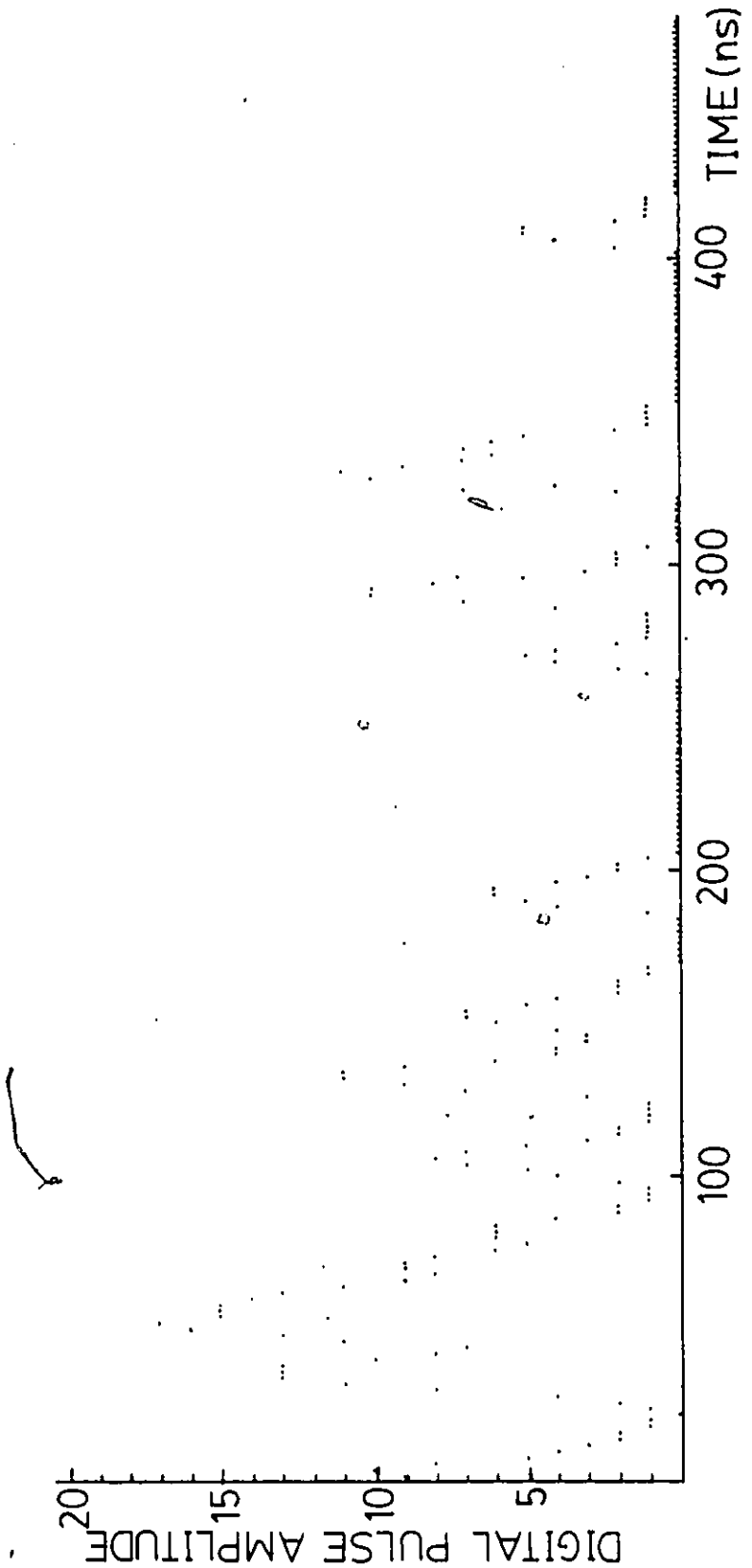

Fig. 9 Typical digitized photomultiplier pulses following a single laser pulse. Time equal to zero corresponds to the peak of the laser pulse.

The Biomation was checked for linearity and time calibration using a Berkeley Nucleonics Corporation Digital Delay Generator model 7010 and a Fluke Counter/Timer model 1953A. The delay generator was found to be stable to 1 part in 10^7 tested over 1 second intervals during the entire calibration time on the 10 MHz pulse frequency range. No error in the time calibration nor any nonlinearity could be measured on either the 2 or 5 ns per channel settings over the full scan of 1024 channels.

V. EXPERIMENTAL PROCEDURE

Before data collection, the fluorescence cell at normal operating temperature was opened to the vacuum system for at least 15 minutes to allow any contaminants which may have outgassed from the cell walls to escape. If data collection continued for longer than 6 hours it was interrupted for an additional 15 minute evacuation. During data collection, the stopcock between the cell and vacuum system remained closed. The temperature of the cell sidearm and body were checked periodically and were not changed throughout the experiment. All electronics including P.M. tube were at operating settings at least 30 minutes prior to data collection for thermal stabilization. The dye laser grating angle was roughly adjusted using the grating equation for Littrow configuration in order that the laser output wavelength correspond to the two-photon transition from the ground state to the level being selectively excited. The laser dyes were mixed at the concentrations specified in the Exciton laser dye catalogue and then adjusted if necessary in order to maximize the power output for the particular spectral range used. The monochromator was then set to the wavelength corresponding to the transition to be observed in fluorescence. The dye laser grating was then further adjusted onto the centre of the absorption by observing the digitized P.M. signal from the Biomation displayed on a C.R.T. The laser beam steering, beam diameter reducing optics into the cell and focusing optics into the monochromator were then adjusted along with the monochromator wavelength setting in order to achieve maximum

fluorescence signal. The linear analyser (linearly polarizing film) and short pass filter located directly in front of the monochromator input were adjusted if necessary.

The dye laser spectral bandwidth was measured using a monitor etalon and its output power was monitored before and throughout the data collection. The dye laser power was kept below about 2.5 mJ per pulse in order to prevent stimulated emission which had been noticed to alter the fluorescence decay signal. When the laser power dropped significantly below the normal operating value the data collection would be briefly interrupted for a change to fresh dyes. During data collection, it was found that the laser grating angle and hence output wavelength would rarely need adjustment due to the relative widths of the laser spectral output and the absorption line.

The microcomputer which controlled the Biomation automatically halted the data collection when the accumulated signal amplitude in its memory reached a predetermined value based on the required counting statistics. Upon finishing the data collection for a particular energy level, the data was printed, plotted and transferred to magnetic disk for analysis at a later time by a modified multi-exponential fitting computer program written by P.C. Rogers[30] at the M.I.T.

VI. RESULTS AND DISCUSSION

The experimental results quoted in Table 1 were found from data obtained at a Cs vapour pressure of about 2×10^{-6} torr with an undetermined background gas pressure of about 3×10^{-7} torr. At these pressures, using the collisional cross-sections of Deech et al.[12], collisional processes will effect the measured lifetimes by less than the statistical uncertainty obtained in the computer program exponential fitting procedure. The systematic errors in pressure and temperature measurements are small and will have a relatively negligible effect on the lifetimes measured.

Lifetime values given in Table 1 are the average of all values obtained from data for each energy level measured. The corresponding error given with each lifetime is four times the typical sigma value, the statistical uncertainty, that was obtained by the exponential fitting computer program. This range of uncertainty was found to encompass all fitted lifetimes or overlap with their 4σ uncertainty.

Example of single sets of data for the energetically lowest and highest ns $^2S_{1/2}$ and nd $^2D_{5/2}$ levels measured, plotted in semi-log fashion, are shown in figures 10(a) through (d). A typical set of data would have an initial maximum accumulated signal amplitude of about 65,000 corresponding to 6,500 photons if the mean amplified P.M. pulse amplitude equals a digitised count of 10. A few periods of modulation of unknown origin at about 17 MHz could be seen on the 7d $^2D_{5/2}$ and 7d $^2D_{3/2}$ data.

Some of the data obtained had residual quantum beat modulation at hyperfine frequencies. An example of this is

TABLE 1

Lifetimes of the levels $ns\ ^2S_{1/2}$ for n = 9 to 15 and $nd\ ^2D_{3/2,5/2}$ for n = 7 to 15. The $7p\ ^2P_{3/2}$ lifetime was found using closed cell data and linearly extrapolating to zero Cs vapour pressure.

Level	Natural Radiative Lifetime (ns)		
	This Experiment	Other Experiments	Coulomb[23] Approx.
$7d\ ^2D_{3/2}$	89±1	98±10[14], 89±4[15]	
$^2D_{5/2}$	89±1	88±9[14]	107
$8d\ ^2D_{3/2}$	141±2	148±3[34], 152±3[12], 154±5[15]	
$^2D_{5/2}$	145±3		168
$9d\ ^2D_{3/2}$	218±3	208±2[34]; 218±4[12]	
$^2D_{5/2}$	217±4		257
$10d\ ^2D_{3/2}$	315±3	310±3[34], 311±6[12]	
$^2D_{5/2}$	321±4		376
$11d\ ^2D_{3/2}$	417±5	428±12[12]	
$^2D_{5/2}$	420±7		529
$12d\ ^2D_{3/2}$	566±11	561±18[12]	
$^2D_{5/2}$	586±11		722
$13d\ ^2D_{3/2}$	746±7	741±22[12]	
$^2D_{5/2}$	768±6		958
$14d\ ^2D_{3/2}$	933±10	980±30[12]	
$^2D_{5/2}$	946±12		1242
$15d\ ^2D_{5/2}$*	1098±12		1578
$9s\ ^2S_{1/2}$	159±3	147±15[14], 160±8[15], 167±3[12]	177
$10s\ ^2S_{1/2}$	265±4	260±12[13], 270±5[12]	293
$11s\ ^2S_{1/2}$	403±4	343±22[13], 411±8[12]	455
$12s\ ^2S_{1/2}$	573±7	545±30[13], 571±15[12]	668
$13s\ ^2S_{1/2}$	777±8	754±35[12]	942
$14s\ ^2S_{1/2}$	1017±20	959±50[12]	1282
$15s\ ^2S_{1/2}$*	1323±20		1698
$7p\ ^2P_{3/2}$	133±5	130±4[31], 134.5±2.8[32], 136±4[33]	128

* The uncertainty given with the lifetime of these levels is not expected to be as reliable as the other values given.

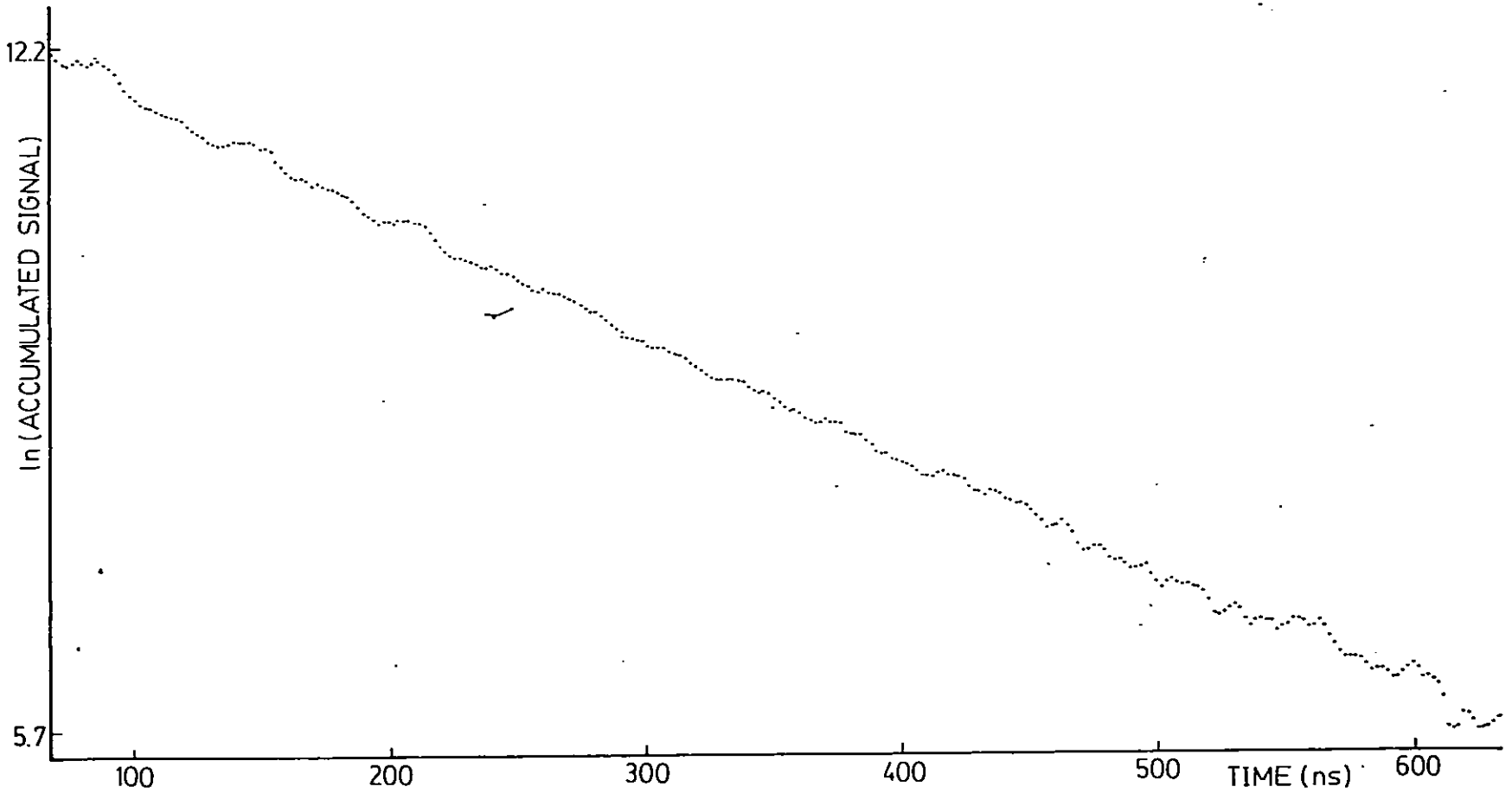

Fig. 10(a)

Fig. 10(a) to 10(d) Semi-log plots of data obtained from the transitions from 7d $^2D_{5/2}$, 15d $^2D_{5/2}$, 9s $^2S_{1/2}$ and 15s $^2S_{1/2}$ to 6p $^2P_{3/2}$ respectively.

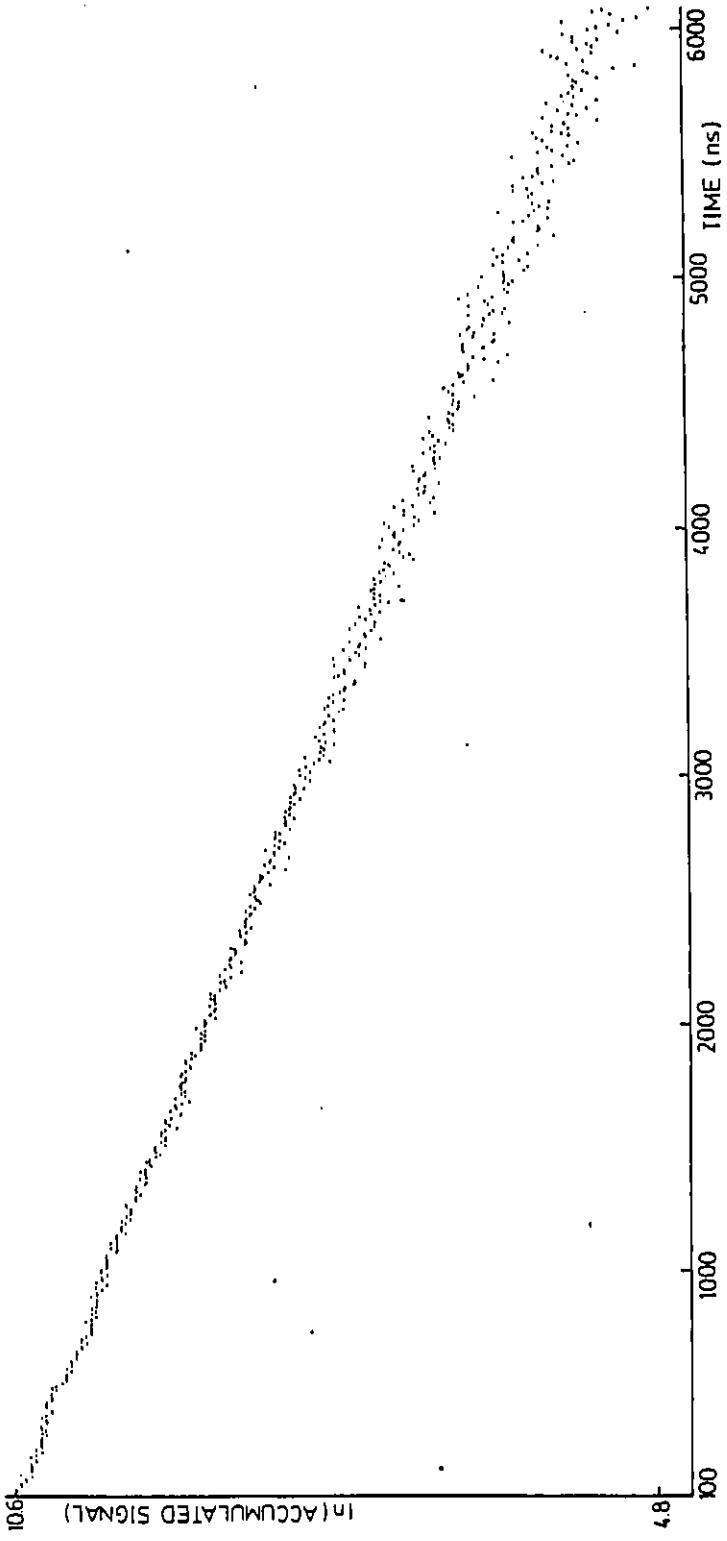

Fig. 10(b) Data from transition 15d $^2D_{5/2}$ to 6p $^2P_{3/2}$.

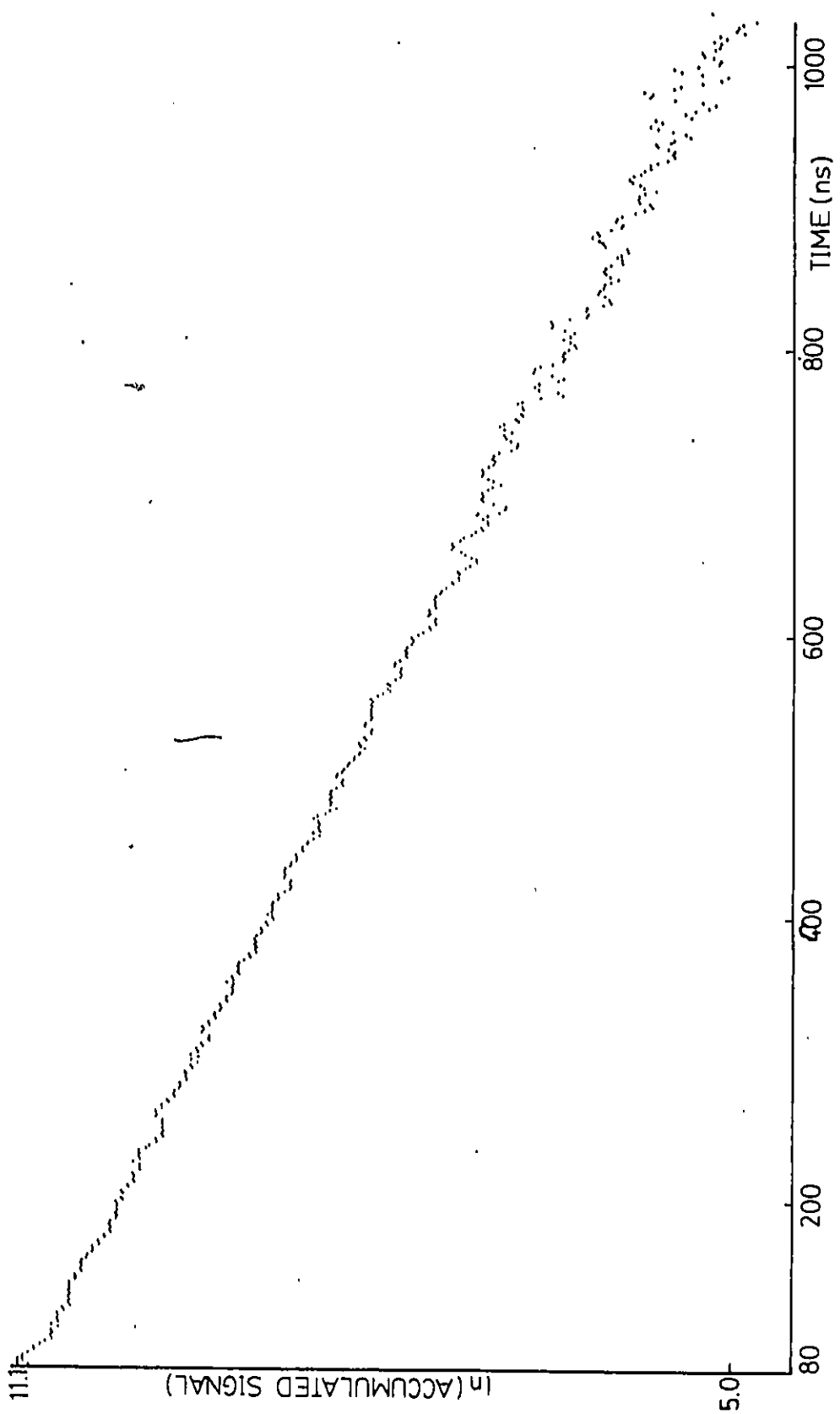

Fig. 10(c) Data from transition $9s\ ^2S_{1/2}$ to $6p\ ^2P_{3/2}$.

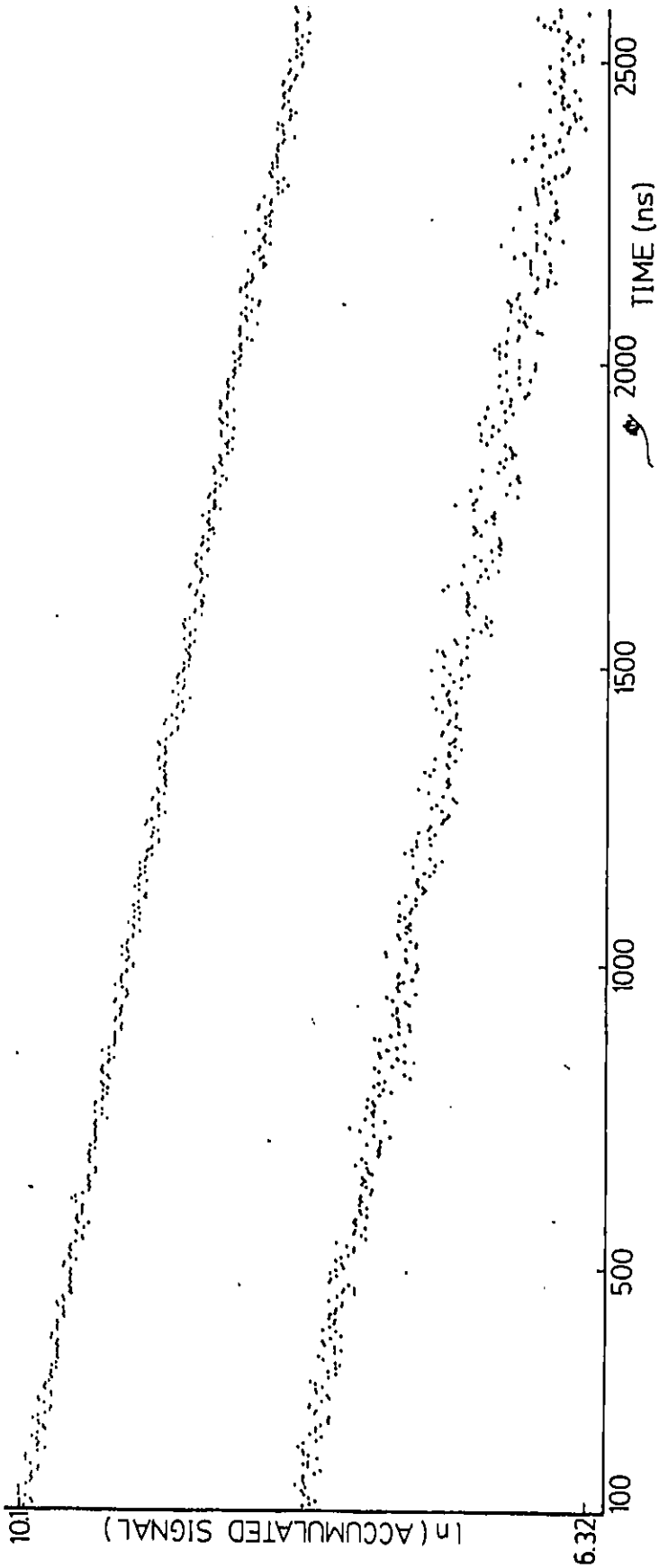

Fig. 10(d) The lower curve for this data from the transition $15s\ ^2S_{1/2}$ to $6p\ ^2P_{3/2}$ is a continuation in time of the upper curve.

shown in figure 11 for the transition 10d $^2D_{5/2}$ + 6p $^2P_{3/2}$. Although small in amplitude, this effect caused the computer program analysis of some data to be more difficult, thus causing an increased uncertainty in some lifetime values obtained. The linear analyser used at the well known "magic angle" of 54.7 degrees[34] did suppress the modulation but did not eliminate it entirely. Deech et al.[34] also observed residual modulation when using a linear analyser at 54.7° and attributed it to a "departure from ideal geometric conditions". Examples of how the linear analyser affected the signal are shown in figures 12(a), (b) and (c) for the transition 8d $^2D_{5/2}$ to 6p $^2P_{3/2}$. Figure 12(c) also shows a simulated fluorescence decay for the above transition with damped modulation due to hyperfine splitting. This curve has the form

$$\alpha e^{-At} + \beta \cos \omega t \; e^{-Bt}$$

with $\alpha = 43{,}500$, $\beta = 35{,}000$, $\omega = 2\pi$ (4.5 MHz), $A = (134 \text{ ns})^{-1}$ and $B = (70 \text{ ns})^{-1}$. In this crude simulation it was found that it was necessary to damp the modulation at about twice the rate as the radiative decay of the population. Deech et al[12] also found that at higher values of n the modulation was damped more rapidly than the population.

Two effects were observed under conditions of high laser power. One was the rapid initial decay in the fluorescence time

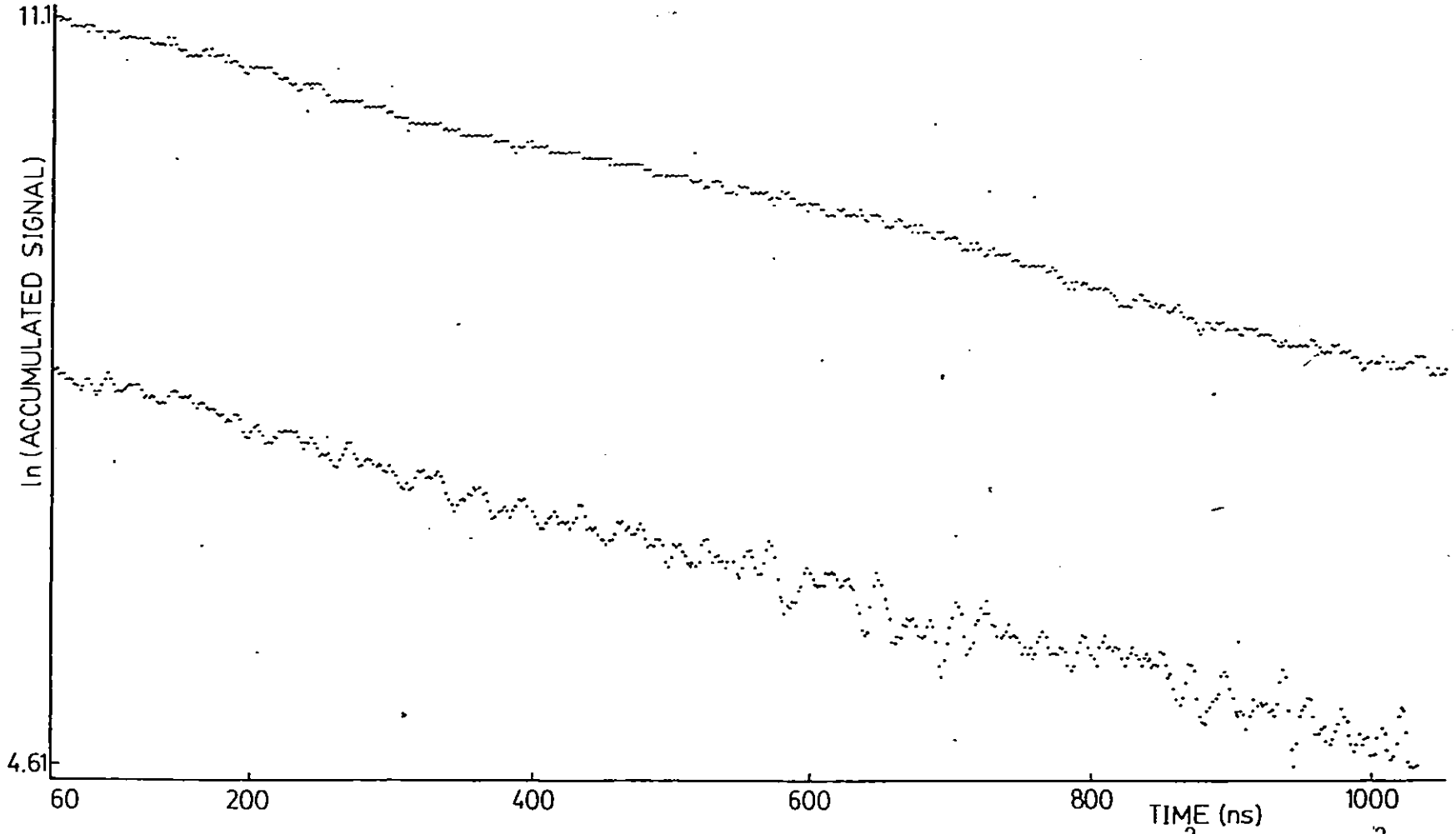

Fig. 11 Semi-log plot of the accumulated signal in the transition 10d $^2D_{5/2}$ to 6p $^2P_{3/2}$ using a linear analyser at 54.7 degrees. Residual modulation is apparent at about 1.8 MHz corresponding to the hyperfine splitting between either F = 5 and F = 4 (2 MHz) or F = 4 and F = 3 (1.6MHz) using the value -0.4 for the magnetic dipole coupling constant given by Svanberg and Tsekeris[35] and the interval rule for hyperfine level separations. The lower curve is a continuation in time of the upper curve.

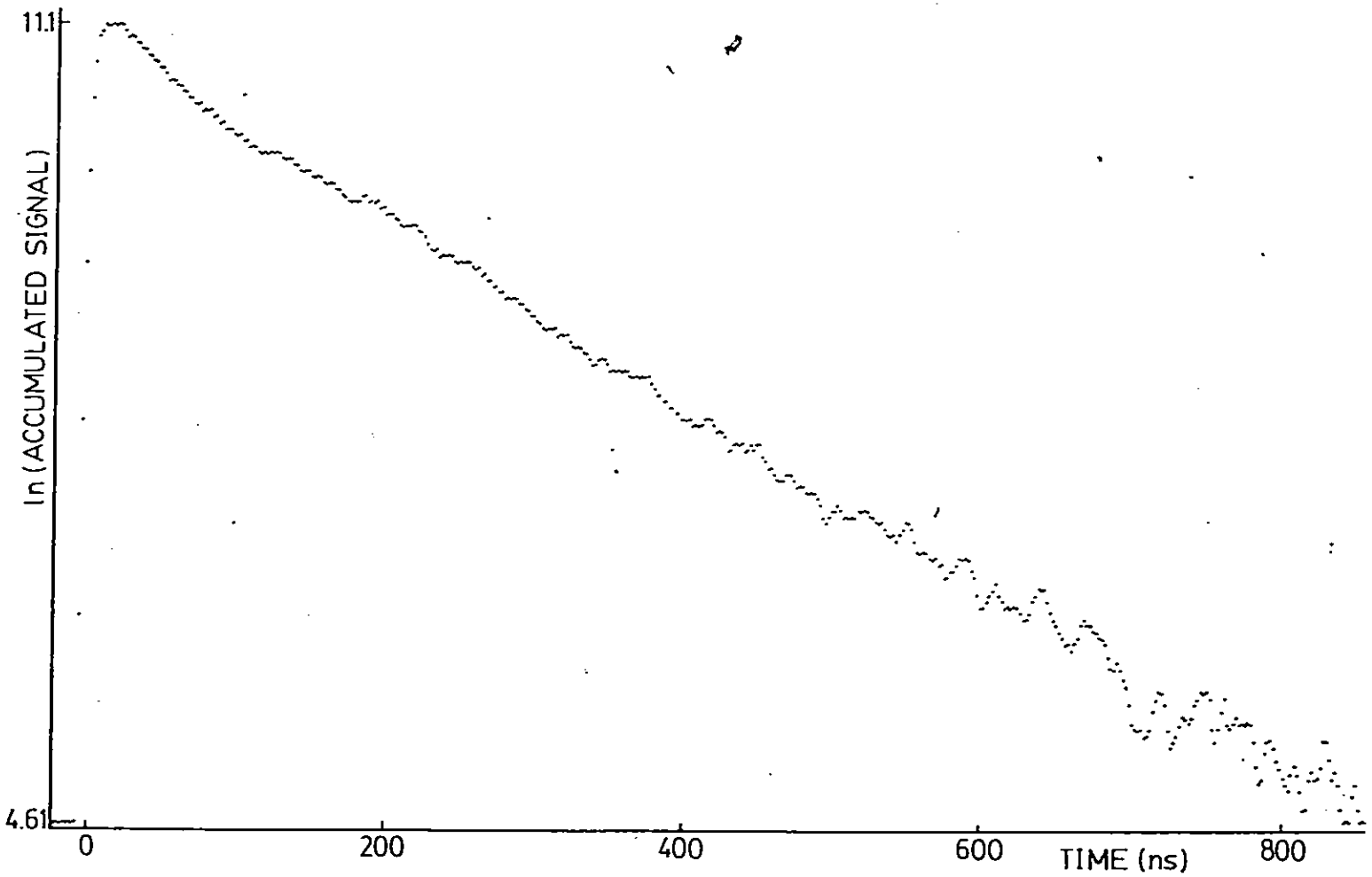

Fig. 12(a) A semi-log plot of the accumulated fluorescence signal from the transition 8d $^2D_{5/2}$ to 6p $^2P_{3/2}$ not using a linear analyser. A small amount of non-linearity can be noticed due to modulation near the beginning of the decay.

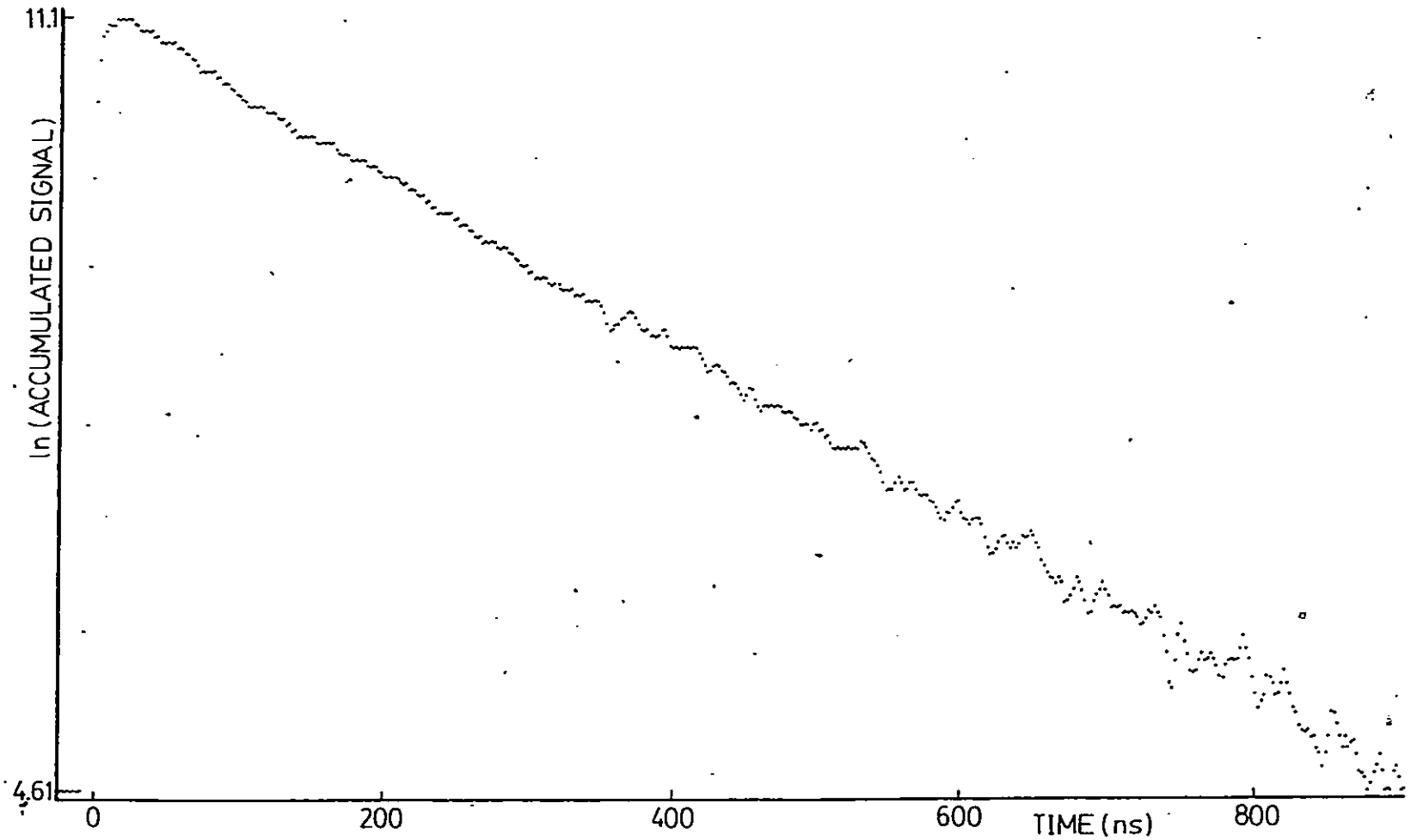

Fig. 12(b) The same type of plot as in 12(a) only a linear analyser is used at an angle of about 55 degrees to the laser polarization. This data shows the minimum modulation of the three figures (a), (b) and (c).

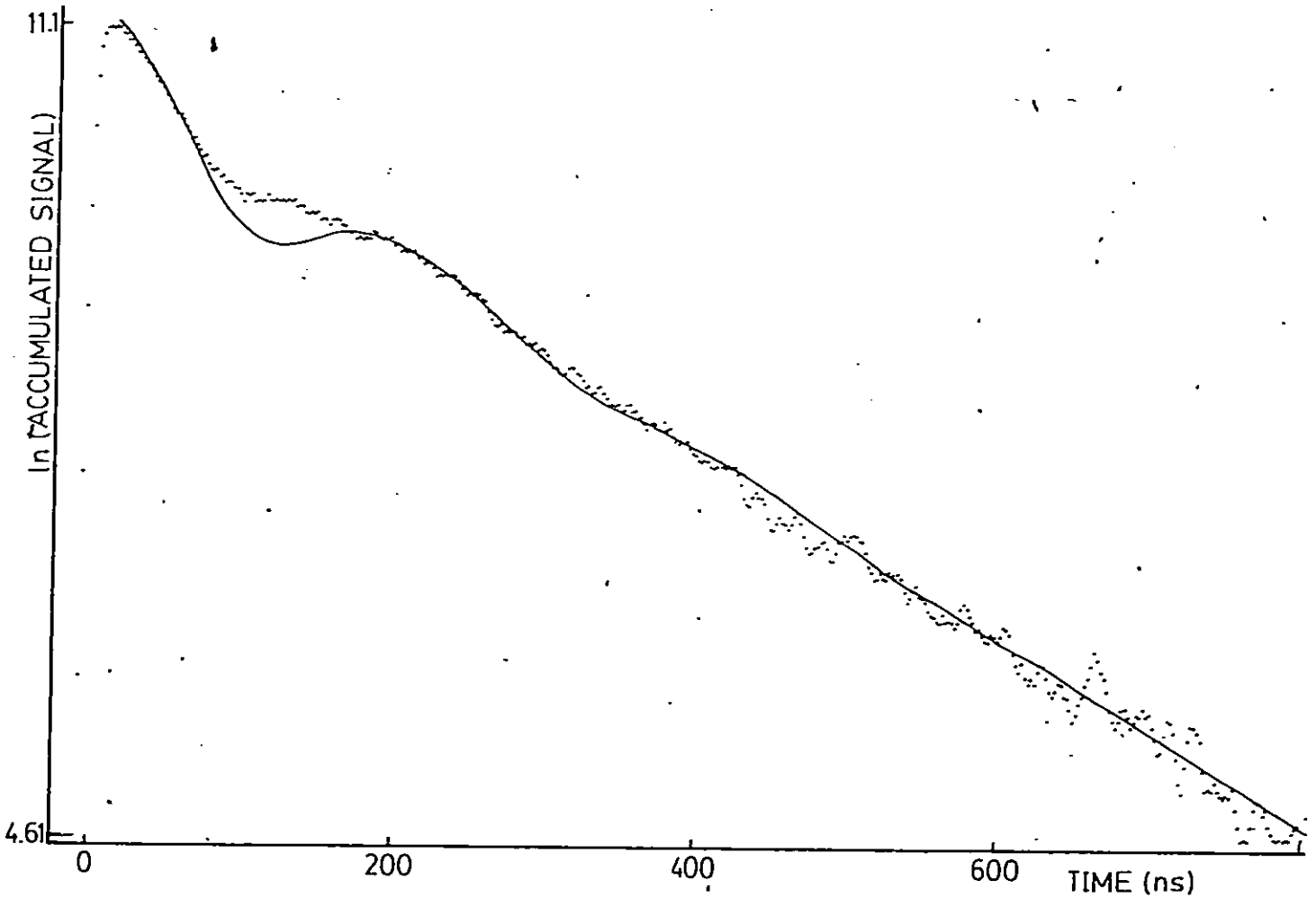

Fig. 12(c) The data for this plot was accumulated with a linear analyser at zero degrees placed in the path of the fluorescence. The modulation is expected to be a maximum for this angle as it was found to be. The solid line is a simulated signal with damped modulation added at a hyperfine interval frequency of 4.5 MHz corresponding to the F = 5, F = 4 energy separation of the 8d $^2D_{5/2}$ level using the magnetic dipole coupling constant given by Svanberg and Tsekeris[35] and using the hyperfine interval rule.

dependence for a transition out of the selectively excited level and the other was the rapid increase in signal for transitions out of non-laser excited levels which were energetically near the excited level. One explanation of this is that stimulated emission occurred from the excited level to nearby radiatively connected levels. Immediately after the laser pulse, there will be a total population inversion between these levels which are coupled by long transition wavelengths which are favourable conditions for stimulated emission. Transitions from the levels $5f\ ^2F_{7/2}$, $7d\ ^2D_{5/2}$, $9p\ ^2P_{3/2}$, $8s\ ^2S_{1/2}$ and $9s\ ^2S_{1/2}$ were measured and were found to show a peak in their fluorescence yield within 30 ns of the laser pulse maximum when selectively exciting the $8d\ ^2D_{5/2}$ level at high laser output powers. The other members of the fine level pairs were also observed to be populated relatively quickly although transitions out of these levels were not measured. Using spontaneous transition rates calculated by Gounand[23] and rate equations coupling the levels, it was found from calculations done in Appendix 5, that the levels directly connected by radiative transitions from the excited level from which transitions were measured could not have a maximum in their fluorescence decay before more than 100 ns after the laser pulse. The observed effect could therefore not be due to spontaneous transition rates. During data collection for lifetime analysis, the laser power was limited so that the above effects would not be observed.

On infrequent occasions, fluorescence was detected in transitions, especially 6p $^2P_{3/2}$ to 6s $^2S_{1/2}$ (lowest P level to the ground state), when the dye laser was being tuned between energetically higher levels to be excited. This signal was noticed to have multiple components and to peak quite late after the laser pulse in the transitions measured. This effect was not studied in detail but has been attributed to three-photon resonant and non-resonant ionization and its subsequent recombination and radiative cascade. Reduction in dye laser output power and bandwidth was found to reduce if not eliminate this effect.

All lifetime values quoted in Table 1 for this work were found using an open cell except for the 7p $^2P_{3/2}$ lifetime which was found by linear extrapolation of closed fluorescence cell data to zero density, as can be seen in figure 13. A linear fit was performed on the data since by Milne's theory of radiation trapping[17,37] the lifetime should, at low vapour densities, increase linearly with vapour pressure. This cell was abandoned since lifetime measurements on levels of higher principal quantum number showed multi-exponential collisional effects which were due to an undetermined background gas pressure, a result of diffusion through the cell walls.

All lifetimes measured for ns $^2S_{1/2}$ levels agree with at least one of the referenced values except for 15s $^2S_{1/2}$ where no reference value could be found. The nd ^2D_J lifetimes agree satisfactorily with the referenced values for J = 3/2, while

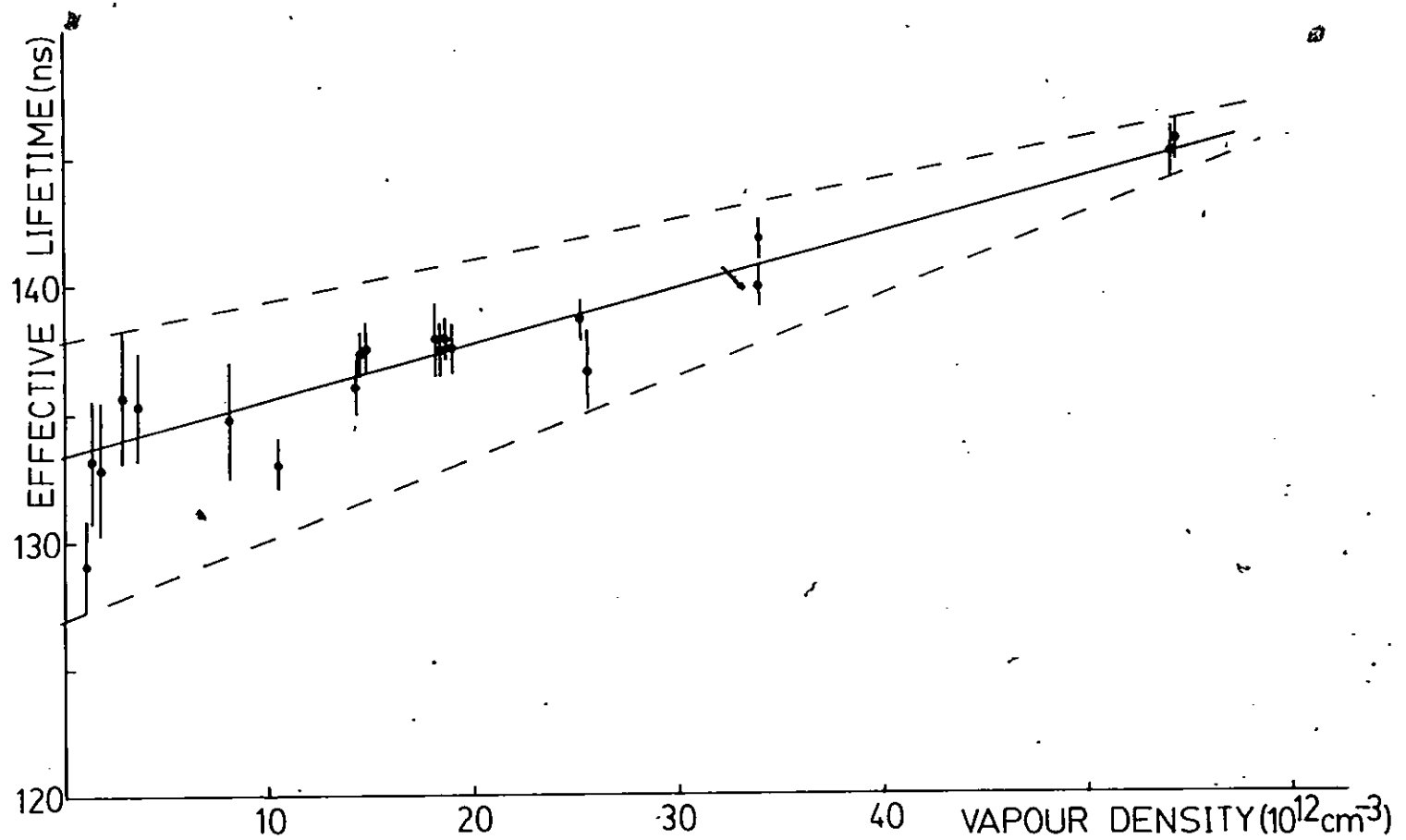

Fig. 13 $7p\ ^2P_{3/2}$ effective radiative lifetime versus Cs vapour density using a sealed fluorescence cell. A linear regression fit gives the zero density lifetime as approximately 133±5ns which is in agreement with the values from references 31, 32 and 33.

only one referenced value could be found for any of the J = 5/2 levels and is in good agreement with the measured value. The data obtained for the 15d ^2D_J levels did not give consistent values for the computer fitted lifetimes, although a value for the 15d $^2D_{5/2}$ level is quoted in Table 1. This value was considered as being the most accurate because it had the most agreement with other data obtained in this experiment and the relative magnitude of this lifetime to its Coulomb approximation value was similar to the other measured lifetimes and their respective Coulomb approximation values. It is possible that the lifetimes of the 15d ^2D_J levels as well as the 15s $^2S_{1/2}$ level could have been substantially effected by the passage of excited atoms out of the region of observation in the fluorescence cell which could shorten their measured lifetimes. There was no observed shortening of other ns $^2S_{1/2}$ level lifetimes of comparable magnitude though, implying the absence of this effect.

Differences between the lifetimes of levels of each fine structure pair were small as expected. The largest difference was about 3.5 percent for the 12d ^2D fine structure pair, the lifetimes of which had a statistical uncertainty of about half of this difference. For the energetically lower levels, these lifetime differences were about equal to or less than the magnitude of the statistical uncertainty which was 2 percent or less.

Using Warner's[6] gf values (where g is a statistical weight and f is an absorption oscillator strength), which were

calculated using the Coulomb approximation allowing for spin-orbit configuration mixing, the spontaneous emission coefficient ratio for the 8d ^2D_J levels was calculated to be $A_{J=5/2}:A_{J=3/2} \approx 1.14$ (see appendix 1). Using f values calculated by Lindgard and Nielsen[22], who also used the Coulomb approximation but without spin-orbit perturbation, the ratios $A_{J=5/2}:A_{J=3/2}(8d\ ^2D_J) \approx 0.98$ and $A_{J=5/2}:A_{J=3/2}(10d\ ^2D_J) \approx 1.05$ were calculated in appendix 6 in a manner similar to that given by Fermi[1]. The latter calculations take into account spin-orbit configuration mixing between configurations of the same angular quantum numbers as the levels whose A ratios were calculated. They also consider transitions to levels within various np and nf configurations but do not consider these levels to be perturbed by the spin-orbit interaction in order to simplify calculations.

The poor agreement between the calculated A coefficient ratios themselves and the measurements from this experiment show the need for a better theoretical treatment of the effects causing lifetime differences within configurations of higher energy and angular momentum. Further measurements with increased accuracy along with measurements of series of levels are necessary in order to be able to measure the small spin-orbit perturbation of lifetimes and to find the relative magnitude of this effect on different configurations and within different atomic systems.

APPENDIX 1

Below are listed spontaneous emission coefficients $A(8d\ ^2D_{3/2})$ and $A(8d\ ^2D_{5/2})$ from theoretical calculations. Warner includes spin-orbit configuration mixing whereas the others do not.

$A(8d\ ^2D_{3/2})$ x 10^{-6}				To	$A(8d\ ^2D_{5/2})$ x 10^{-6}
Warner[6]	Anderson[21] & Zilitis	Lindgard[22] & Nielsen	Gounand[23]		Warner[6]
3.547	7.51	4.032	3.80	6p	4.176
1.164	2.27	1.337	1.31	7p	1.398
(0.50)	0.840	0.516	0.499	8p	(0.50)
			0.00515	9p	
0.145	0.0825	0.114	0.115	4f	0.121
0.256	0.141	0.203	0.204	5f	0.202
5.61	10.9	6.202	5.93	Total	6.40

Bracketed values are estimates.

From Warner's calculations

$$\frac{A(8d\ ^2D_{5/2})}{A(8d\ ^2D_{3/2})} = 1.14$$

APPENDIX 2

The following calculation gives an approximate effective lifetime of the 6p ^2P_J levels in Cs due to trapping (see Mitchell and Zemansky[17] for details).

The absorption coefficient at line centre, k_o, is given by

$$k_o = \frac{(\ell n 2)^{1/2}\ \lambda_o^{\,2}}{4\pi^{3/2}\ \Delta\nu_D}\ g_2/g_1\ \ N/\tau \quad \text{(eq. 35, p. 100 in ref. 17)}$$

where λ_o is the transition wavelength, $\Delta\nu_D$ is the Doppler width, g_2 and g_1 are statistical weights, N is the ground state density and τ is the natural radiative lifetime.

$$\Delta\nu_D = \frac{2\nu_o}{c}\left(\frac{2RT\ell n 2}{M}\right)^{1/2} \sim 425\ \text{MHz} \quad \text{(eq. 33, p. 99 in ref. 17).}$$

The effective lifetime due to trapping is given by

$$\tau' = \tau\ [1 + (\frac{\bar{k}\ell}{y'})^2] \quad \text{(eq. 153, p. 231 in ref. 17)}$$

where ℓ is the depth of trapping, $\bar{k}\ell$ is the equivalent opacity given by

$$\bar{k}\ell = 0.675\ k_o\ell \quad \text{for } k_o\ell \leq 1.00$$

and y' is the first root of $\tan y = \frac{\bar{k}\ell}{y}$.

For $\tau \approx 35$ ns, $g_2/g_1 = 2$, $\lambda_o = 852$ nm, $N = 6 \times 10^{10}$ cm^{-3} and $\ell = 3$ mm it is found that $k_o \approx 57$ m^{-1}, $\bar{k}\ell \approx 0.115$, $y' \approx 0.333$ and $\tau' \approx 39$ ns.

Therefore, re-absorption of radiation by the ground state causing a re-population of a 6p ^2P_J level changes the 6p ^2P_J lifetime by about 11%.

Since the population of a 6p ^2P_J level would be much less than the ground state population N, re-absorption from these levels to the selectively excited state will insignificantly effect the measured lifetimes of the excited S and D levels.

APPENDIX 3

The mean free path for particles with a Maxwellian velocity distribution is given by

$$\ell=(\sqrt{2}\ N\ \pi r^2)^{-1}$$

where N is the Cs vapour density and r is the atomic radius.

During the experiment, the fluorescence cell sidearm temperature was 302 Kelvins, the cell body temperature was 328 Kelvins and N was approximately 6×10^{10} cm^{-3} using the data of Nesmeyanov[24]. The ionic radius of Cs, r, given in the Science Data Book[36] is approximately 1.67×10^{-8} cm. Using the above, ℓ is about 1.3×10^{4} cm, much larger than the region of observation.

It is also necessary to calculate the distance of travel during a typical observation period. Using the fluorescence cell body temperature, the atomic weight of Cs and the expression for the mean particle velocity

$$\bar{V} = \left(\frac{8RT}{\pi M}\right)^{1/2}$$

$\bar{V}$ is calculated to be approximately 2.52×10^{4} cm s^{-1}.

For an observation period of 2 μs, a Cs atom could travel a distance of approximately 0.5 mm. Since the detection apparatus slit size used for an observation period of this magnitude was 1 mm and the diameter of the laser beam in the fluorescence

cell was about 2 mm, the thermal migration of excited atoms should not significantly affect the typical magnitude of lifetimes measured.

APPENDIX 4

This calculation shows the negligible effect of collisions between excited and ground state Cs atoms, at the vapour density used, on the measured lifetimes.

The temperature of the fluorescence cell sidearm which controlled the Cs vapour pressure was kept at 302±1 Kelvins. Using the empirical vapour pressure formula

$$\log_{10}P[\text{torr}] = 8.22 - \frac{4.006\times10^{3}}{T[K]} - 6.019\times10^{-4}T[K] - 1.962\times10^{-1}\log_{10}T[K],$$

given by Nesmeyanov[24] for liquid Cs, the vapour pressure was calculated to be $P \approx 1.94\times10^{-6}$ torr. Using the temperature of the fluorescence cell body $T_o \approx 328$ Kelvins and the ideal gas law

$$N[\text{cm}^{-3}] \approx 9.656\times10^{18}\,\frac{P[\text{torr}]}{T_o[K]},$$

the vapour density was calculated to be $N \approx 5.70\times10^{10}$ cm^{-3}. The mean relative velocity of colliding Cs atoms given by equation (9) is $\bar{V}_r \approx 3.23\times10^{4}$ cm s^{-1} giving $N\bar{V}_r \approx 1.84\times10^{15}$ cm^{-2}s^{-1}. Using $N\bar{V}_r$, the collision cross sections given by Deech et al.[12] and the equations for collisional mixing between two levels given in the Theory, the values in the table below were calculated.

The lifetimes of the two collisional components τ_- and τ_+ are thus in good agreement with τ for the range of levels measured. The largest difference is obtained for the energetically highest D level measured and is less than two percent, smaller

TABLE FOR APPENDIX 4

Level	Approx. mean lifetime from this exp't τ[ns]	Decay Constant $A = \tau^{-1}$[ns^{-1}]	Mixing Cross Section $Q_{3/2\to5/2}$[cm^2]	Mixing Cross Section $Q_{5/2\to3/2}$[cm^2] Given by Eq. 10	$\tau_{(-)}=\lambda_{(-)}^{-1}$ [ns]	$\tau_{(+)}=\lambda_{(+)}^{-1}$ [ns]	$X_{(+)}:X_{(-}$
7d ^2D	89	1.12×10^{-2}	$<10\times10^{-14}$	$<7\times10^{-14}$			4:6
8d ^2D	143	6.99×10^{-3}	$<10\times10^{-14}$	$<7\times10^{-14}$	143	143	4:6
9d ^2D	218	4.59×10^{-3}	$50\times10^{-14}\pm50$	33×10^{-14}	218	218	4:6
10d ^2D	318	3.14×10^{-3}	$60\times10^{-14}\pm50$	40×10^{-14}	318	318	4:6
11d ^2D	419	2.39×10^{-3}	$90\times10^{-14}\pm60$	60×10^{-14}	419	418	4:6
12d ^2D	576	1.74×10^{-3}	$130\times10^{-14}\pm50$	87×10^{-14}	576	575	4:6
13d ^2D	757	1.32×10^{-3}	$240\times10^{-14}\pm80$	160×10^{-14}	757	753	4:6
14d ^2D	940	1.06×10^{-3}	$320\times10^{-14}\pm100$	213×10^{-14}	940	931	4:6
15d ^2D	1098	9.11×10^{-4}	$460^{*}\times10^{-14}$	$308^{*}\times10^{-14}$	1098	1081	4:6
9s ^2S	159	6.29×10^{-3}	$<10\times10^{-14}$	2.5×10^{-14}	159	159	2:14
13s ^2S	777	1.29×10^{-3}	$190\times10^{-14}\pm70$	48×10^{-14}	777	774	2:14

* Estimated cross section extrapolated from values of Deech et al.[12]

than this experiment's statistical uncertainty. The amplitude ratio $A_+:A_-$ is given simply by the ratio of the statistical weights of the mixed levels because the lifetimes of the mixed levels were were assumed equal for ease of calculation. If in these calculations the natural lifetimes were assumed to differ within each configuration by 3 percent (as they might due to spin-orbit perturbation), the results would be essentially the same as far as the relative magnitude of the collisional decay components (λ_+ and λ_-) are concerned.

APPENDIX 5

The following rate equation calculations were done in order to show that spontaneous transition rates alone were not responsible for the fluorescence time dependence found in transitions from some levels under conditions of high laser output power.

Consider the following energy level diagram where level 2 is excited directly by the pulsed laser at t = 0 and radiates spontaneously to an energetically lower nearby level 1.

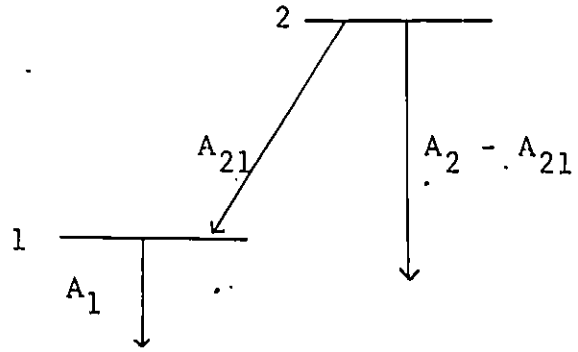

The rate equations for this system of levels are:

$$\dot{N}_2 = -N_2A_{21} - N_2(A_2 - A_{21}) = -N_2A_2 \qquad \text{(i)}$$

$$\dot{N}_1 = -N_1A_1 + N_2A_{21} \qquad \text{(ii)}$$

If the population of level 2 at t = 0 is $N_2(0)$, equation (i) has the solution

$$N_2(t) = N_2(0)\, e^{-A_2 t}$$

Substituting this into equation (ii) and with the additional initial condition $N_1(t = 0) = 0$, the general solution

of (ii) is found to be

$$N_1(t) = \frac{A_{21}N_2(0)}{A_1-A_2}\left(e^{-A_2t}-e^{-A_1t}\right)$$

The peak in the fluorescence yield from level 1 will be at the time t_p when $N_1 = 0$ that is,

when $A_2e^{-A_2t_p} = A_1e^{-A_1t_p}$ which gives $t_p = \frac{\ell n(A_1/A_2)}{A_1-A_2}$. (iii)

We can now estimate the time after the laser pulse at which the fluorescence yield from levels populated by spontaneous decay of the laser excited level should be maximum.

If level 2 is the 8d $^2D_{5/2}$ level and level 1 is either the 5f $^2F_{7/2}$ or 9p $^2P_{3/2}$ levels we obtain, using A values calculated by Gounand[23] and equation (iii), that;

$$A(8d\ ^2D) = A(8d\ ^2D \text{ to } 4f\ ^2F)+A(8d\ ^2D \text{ to } 5f\ ^2F)+A(8d\ ^2D \text{ to } 9p\ ^2P)$$
$$+A(8d\ ^2D \text{ to } 6p\ ^2P)+A(8d\ ^2D \text{ to } 7p\ ^2P)+A(8d\ ^2D \text{ to } 8p\ ^2P)$$
$$\approx 5.93\times10^6\ s^{-1}$$

$$A(5f\ ^2F) = A(5f\ ^2F \text{ to } 5d\ ^2D)+A(5f\ ^2F \text{ to } 6d\ ^2D)+A(5f\ ^2F \text{ to } 7d\ ^2D)$$
$$\approx 1.11\times10^7\ s^{-1}$$

$$A(9p\ ^2P) - A(9p\ ^2P \text{ to } 5d\ ^2D)+A(9p\ ^2P \text{ to } 6d\ ^2D)+A(9p\ ^2P \text{ to } 7d\ ^2D)$$
$$+A(9p\ ^2P \text{ to } 6s\ ^2S)+A(9p\ ^2P \text{ to } 7s\ ^2S)+A(9p\ ^2P \text{ to } 8s\ ^2S)$$
$$\approx 1.60\times10^6\ s^{-1}$$

$t_p(5f\ ^2F) \approx 121$ ns

$t_p(9p\ ^2P) \approx 303$ ns.

Since these levels were found to peak in their fluorescence yield within 30 ns after the laser pulse, another mechanism in addition to spontaneous emission from the selectively excited level must have populated them, probably stimulated emission.

APPENDIX 6

See references by Fermi[1], zu Putlitz[2] and Warner[6] for more theoretical detail..

The ratio of spontaneous emission coefficients for the nd $^2D_{5/2}$ and nd $^2D_{3/2}$ levels can be written as

$$\frac{A(nd\ ^2D_{5/2} \text{ to } n\ell\ ^2L_J)}{A(nd\ ^2D_{3/2} \text{ to } n\ell\ ^2L_J)} = \left(\frac{\lambda_{3/2}}{\lambda_{5/2}}\right)^3 \frac{g_{3/2}}{g_{5/2}} \left(\frac{S_{5/2}}{S_{3/2}}\right) \qquad \text{(i)}$$

where $S_{5/2}$ and $S_{3/2}$ are the total line strengths from the nd $^2D_{5/2}$ and nd $^2D_{3/2}$ levels to $n\ell\ ^2L_J$. $\lambda_{5/2}$ and $\lambda_{3/2}$ are the wavelengths of the strongest transitions from the J = 5/2 and J = 3/2 levels to the nℓ configuration.

The spin-orbit perturbed line strength ratio for the nd $^2D_{5/2,3/2}$ levels is given by

$$\frac{S_{5/2}}{S_{3/2}} = \frac{3}{2}\left[\frac{1 + 2/5 \sum_m \frac{(\Delta_n \Delta_m)^{1/2}}{E_n - E_m}\left(\frac{S_m}{S_n}\right)^{1/2}}{1 - 3/5 \sum_m \frac{(\Delta_n \Delta_m)^{1/2}}{E_n - E_m}\left(\frac{S_m}{S_n}\right)^{1/2}}\right]^2 \qquad \text{(ii)}$$

and is found in exactly the same manner as the expression for the line strength ratio for the np $^2P_{3/2,1/2}$ levels in Fermi's equation (13) using first order perturbation theory for the radial wave functions.

S_m and S_n are the total line strengths of the fine structure level doublets md ^2D_J (the perturbing levels) and

nd ^2D_J (the levels whose A ratio is being calculated).

The ratio of these line strengths can be expressed in terms of the absorption oscillator strengths of the corresponding transitions by,

$$\frac{S_m}{S_n} = \frac{\lambda_m f_m}{\lambda_n f_n} \qquad \text{(iii)}$$

In this way, spin-orbit perturbed transition A ratios were calculated for transitions to energetically lower levels that involved an appreciable branching coefficient. The absorption oscillator strengths calculated by Lindgard and Nielsen[22] were used to compute the line strength ratios.

The ratio of A coefficients for a particular fine structure level pair was then calculated using transition A values of the previous authors and the transition A ratios found from (i), (ii) and (iii). $A(8d\ ^2D_{5/2}):A(8d\ ^2D_{3/2})$ was calculated considering the 5, 6, 7, 9, 10 and 11d configurations to be mixed with 8d and considering transitions to the 6p ^2P, 7p ^2P, 8p ^2P, 4f ^2F and 5f ^2F terms.

$n\ell\ ^2L$	$\sum_n \frac{(\Delta_n\Delta_8)^{1/2}}{E_8-E_n}\left(\frac{S_n}{S_8}\right)^{1/2}$	$\frac{S_{5/2}}{S_{3/2}}$	$\frac{A(8d\ ^2D_{5/2}\text{ to }n\ell\ ^2L)}{A(8d^2\ D_{3/2}\text{ to }n\ell^2L)}$
6p ^2P	0.03478	1.6095	0.971
7p ^2P	0.03524	1.601	0.986
8p ^2P	0.02398	1.574	0.946
9p ^2P	-0.00200	1.494	0.992
4f ^2F	0.10100	1.840	1.240
5f ^2F	0.01700	1.566	1.089

Then,

$$\frac{A(8d\ ^2D_{5/2})}{A(8d\ ^2D_{3/2})} \approx \frac{\begin{array}{l}0.971A(8d\ ^2D \text{ to } 6p\ ^2P)+0.986A(8d\ ^2D \text{ to } 7p\ ^2P)\\ +0.946A(8d\ ^2D \text{ to } 8p\ ^2P)+0.992A(8d\ ^2D \text{ to } 9p\ ^2P)\\ +1.240A(8d\ ^2D \text{ to } 4f\ ^2F)+1.089A(8d\ ^2D \text{ to } 5f\ ^2F)\end{array}}{\begin{array}{l}A(8d\ ^2D \text{ to } 6p\ ^2P)+A(8d\ ^2D \text{ to } 7p\ ^2P)\\ +A(8d\ ^2D \text{ to } 8p\ ^2P)+A(8d\ ^2D \text{ to } 9p\ ^2P)\\ +A(8d\ ^2D \text{ to } 4f\ ^2F)+A(8d\ ^2D \text{ to } 5f\ ^2F)\end{array}}$$

$$\approx 0.981.$$

$A(10d\ ^2D_{5/2}):A(10d\ ^2D_{3/2})$ was calculated considering the 5, 6, 7, 8, 9, 11 and 12d configurations to be mixed with 10 d and considering transitions to the 6, 7 and 8p ^2P and 4, 5, 6 and 7f ^2F terms.

$n\ell\ ^2L$	$\sum_n \frac{(\Delta_n\Delta_{10})^{1/2}}{E_{10}-E_n}\left(\frac{S_n}{S_{10}}\right)^{1/2}$	$\frac{S_{5/2}}{S_{3/2}}$	$\frac{A(10d\ ^2D_{5/2} \text{ to } n\ell\ ^2L)}{A(10d\ ^2D_{3/2} \text{ to } n\ell\ ^2L)}$
6p ^2P	0.0648	1.709	1.040
7p ^2P	0.0538	1.671	1.039
8p ^2P	0.0554	1.677	1.050
4f ^2F	0.1718	2.130	1.424
5f ^2F	0.1270	1.941	1.301
6f ^2F	0.0872	1.789	1.208
7f ^2F	0.0146	1.544	1.076

Then $$\frac{A(10d\ ^2D_{5/2})}{A(10d\ ^2D_{3/2})} \approx 1.05$$

In both cases the difference between the A values and hence lifetimes of the levels within the configuration are 5 percent or less.

BIBLIOGRAPHY

1. E. Fermi: Z. Physik 59, 680-686 (1930).
2. G. Zu Putlitz: Comments on Atom. & Molec. Phys. 51-56 (1969).
3. G. K. Woodgate: Elementary Atomic Structure. (McGraw-Hill Publishing Co. Ltd., Maidenhead, Berkshire, England, 1970), pp. 107-108.
4. C-J. Lorenzen and K. Niemax: J. Phys. B 11, L723-L728 (1978).
5. S. M. Curry, C. B. Collins, M. Y. Mirza et al.: Opt. Commun. 16, 251-255 (1976).
6. B. Warner: Monthly Notices of the R. Astr. Soc., 139, 115-128 (1968).
7. D. W. Norcross: Phys. Rev. A 7, 606-616 (1973).
8. J. C. Weisheit: Phys. Rev. A 5, 1621-1630 (1972).
9. D. Hofsaess: Z. Physik A 281, 1-13 (1977).
10. J. Marek and P. Munster: J. Phys. B 10, L137-L141 (1977).
11. U. Teppner and P. Zimmerman: Astron. & Astrophys. 64, 215-217(1978).
12. J. S. Deech, R. Luypaert, L. R. Pendrill and G. W. Series: J. Phys. B 10, L137-L141 (1977).
13. H. Lundberg and S. Svanberg: Phys. Lett. 56A, 31-33 (1976).
14. J. Marek: Phys. Lett. 60A, 190-192 (1977).
15. J. Marek and R. Ryschka: Phys. Lett. 74A, 51 (1979).
16. L. R. Pendrill: J. Phys. B 10, L469-L475 (1977).
17. A. Mitchell and M. Zemansky: Resonance Radiation and Excited Atoms. (Cambridge University Press, 1934), Chapter IV. §8a and 12b.

18. M. P. Silverman, S. Haroche and M. Gross: Phys. Rev. A 18, 1507-1528 (1978).

19. S. Haroche: Topics in Applied Physics. (Springer-Verlag Pub., 1976, edited by K. Shimoda), Vol. #13, pp. 253-313.

20. S. Haroche, J. A. Paisner and A. L. Schawlow: Phys. Rev. Lett. 30, 948 (1973).

21. E. M. Anderson and V. A. Zilitis: Optics and Spectroscopy, 16, 211 (1964).

22. A. Lindgard and S. E. Nielsen: Atom. Data and Nuc. Data Tables, 19, 533-633 (1977).

23. F. Gounand: J. Physique (Paris) 40, 457-460 (1979).

24. A. N. Nesmeyanov: Vapour Pressure of the Elements. (Academic Press, New York, 1963), Table 2, p. 443.

25. W. L. Wiese: Progress in Atomic Spectroscopy Part B. Edited by W. Hanle and H. Kleinpoppen (Plenum Publishing Corp., 1979).

26. D. Kleppner: ibid.

27. R. Fowler: ibid.

28. P. Braunlich: ibid.

29. C. Tai, W. Happer and R. Gupta: Phys. Rev. A 12, 736-747 (1975).

30. P. C. Rogers: Laboratory of Nuclear Science Technology Report #76. (Massachusetts Institute of Technology, Boston, Massachusetts, 1962).

31. E. Campani, G. Degan and G. Gorini: Lettere al Nuovo Cimento 23, 187-191 (1978).

32. R. W. Schmieder, A. Lurio, W. Happer and A. Khadjavi: Phys. Rev. A 2, 1216-1228 (1970).

33. P. W. Pace and J. B. Atkinson: Can. J. Phys. 53, 937-941 (1975).

34. J. S. Deech, R. Luypaert and G. W. Series: J. Phys. B 8, 1406-1414 (1975).

35. S. Svanberg and P. Tsekeris: Phys. Rev. A 11, 1125-1137 (1975).

36. Science Data Book, edited by R. M. Tennent (Oliver and Boyd, Edinburgh, 1971).

37. E. Milne: Journal of the London Mathematical Society 1, 1 (1926).

VITA AUCTORIS

I was born on November 24, 1956 in Chatham, Ontario, Canada, and lived nearby in Dresden until I was 13 years of age. I then moved near Belle River, Ontario, where I attended Belle River District High School until 1975 when I graduated with an Honours Secondary School Diploma as an Ontario Scholar. In the same year I enrolled at the University of Windsor and after 4 years obtained an Honours B.Sc. in Applied Physics. I then entered the physics graduate study program in 1979 with a University of Windsor Graduate Scholarship. During my 3 years of research toward my M.Sc., I obtained another University of Windsor Graduate Scholarship, summer research assistantships and was aided by a grant from the National Research Council of Canada. Upon completion of this research, I will begin employment at the Herzberg Institute of Astrophysics in Ottawa, Ontario, Canada.